

Lecture 4

From Simulations to Observations

Baojiu Li (ICC, Durham)

Mexican Numerical Simulations School (03-06 Oct 2016)

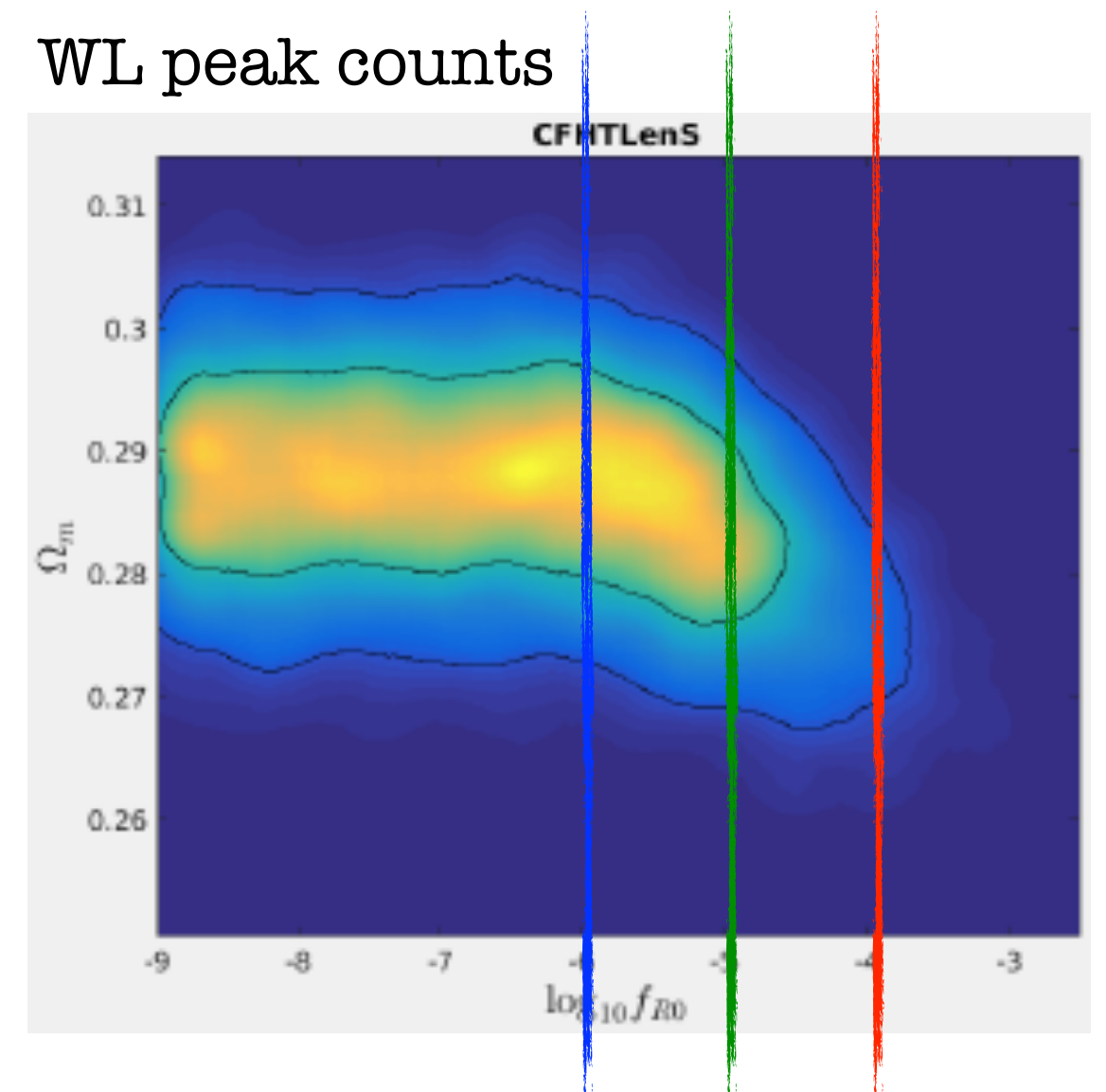
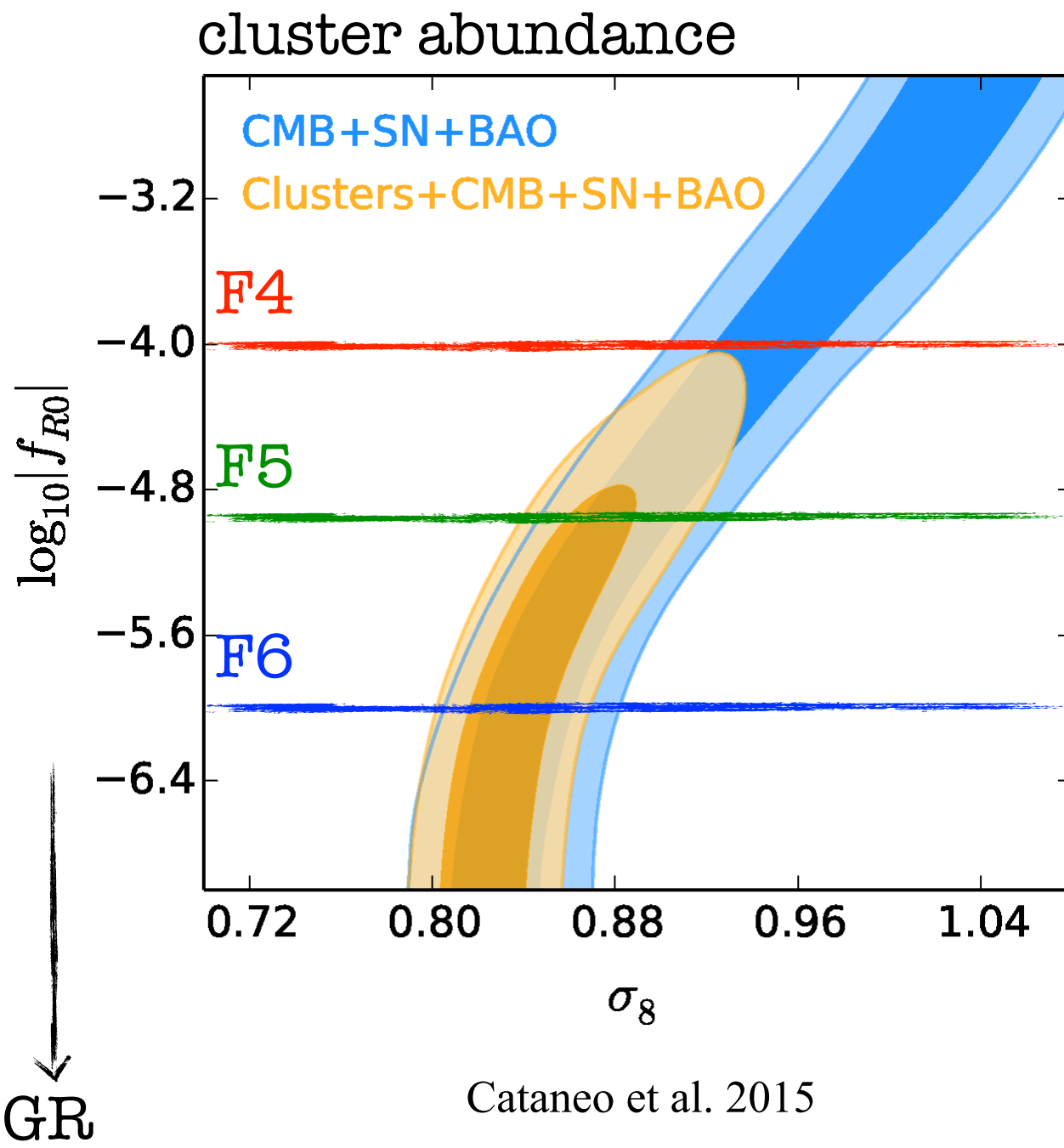
Context

- Cosmology has entered precision era (for many years): (e) BOSS, CFHTLenS, KIDS, DES, ...
- Next decade will see a further flux of greatly improved observations, DESI, eROSITA, Euclid, LSST, ...
- Ideally, we would like to use these observations not just to constrain cosmological parameters of the LCDM scenario, but also to test/exclude nonstandard models.
- This will involve connecting theoretical quantities calculated from the output of N-body (or hydro) simulations to observables.
- Which is not always trivial, and should ideally involve collaborations of theorists, simulators and observers.

This Lecture

- In this lecture, I'll review some recent results of constraining nonstandard models from various groups
- I will divide these into different probes: weak gravitational lensing and clusters of galaxies
- Note:
- Galaxy clustering is also a potentially powerful probe, and is very relevant for DESI. But progress in this has been little so far.
- For each class of probe, there are different observables that can be compared with theoretical predictions

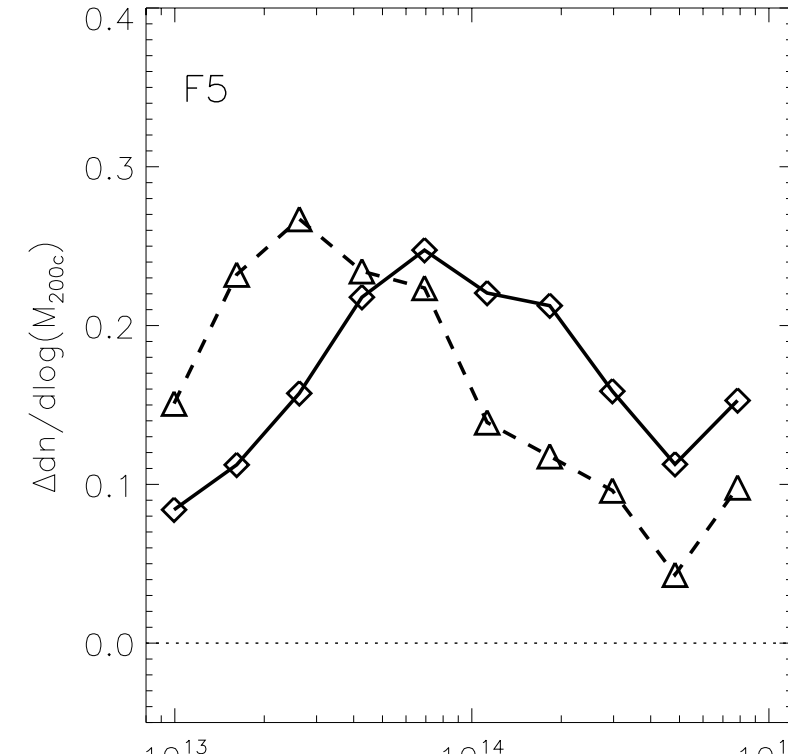
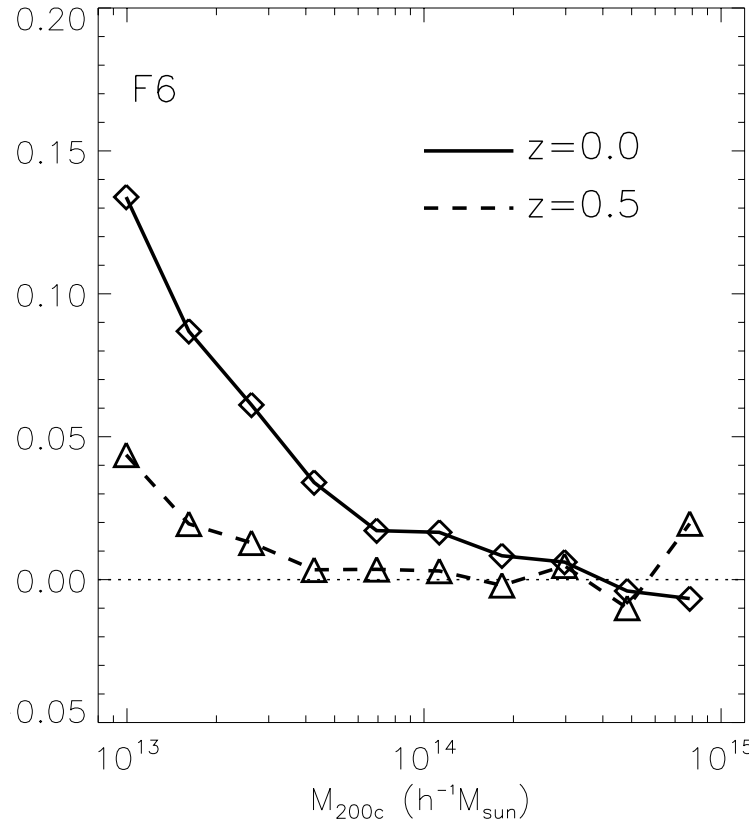
Setting Up the Ground



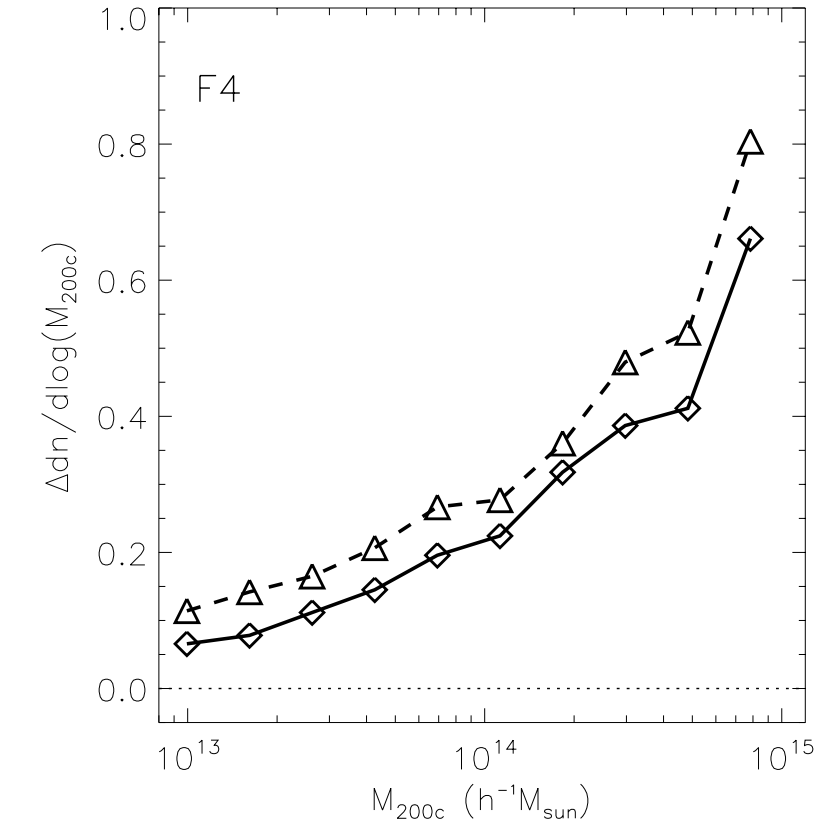
$f(R)$ Gravity - my Lord of Models

Halo mass function diff from GR

varying model parameters



Halo mass



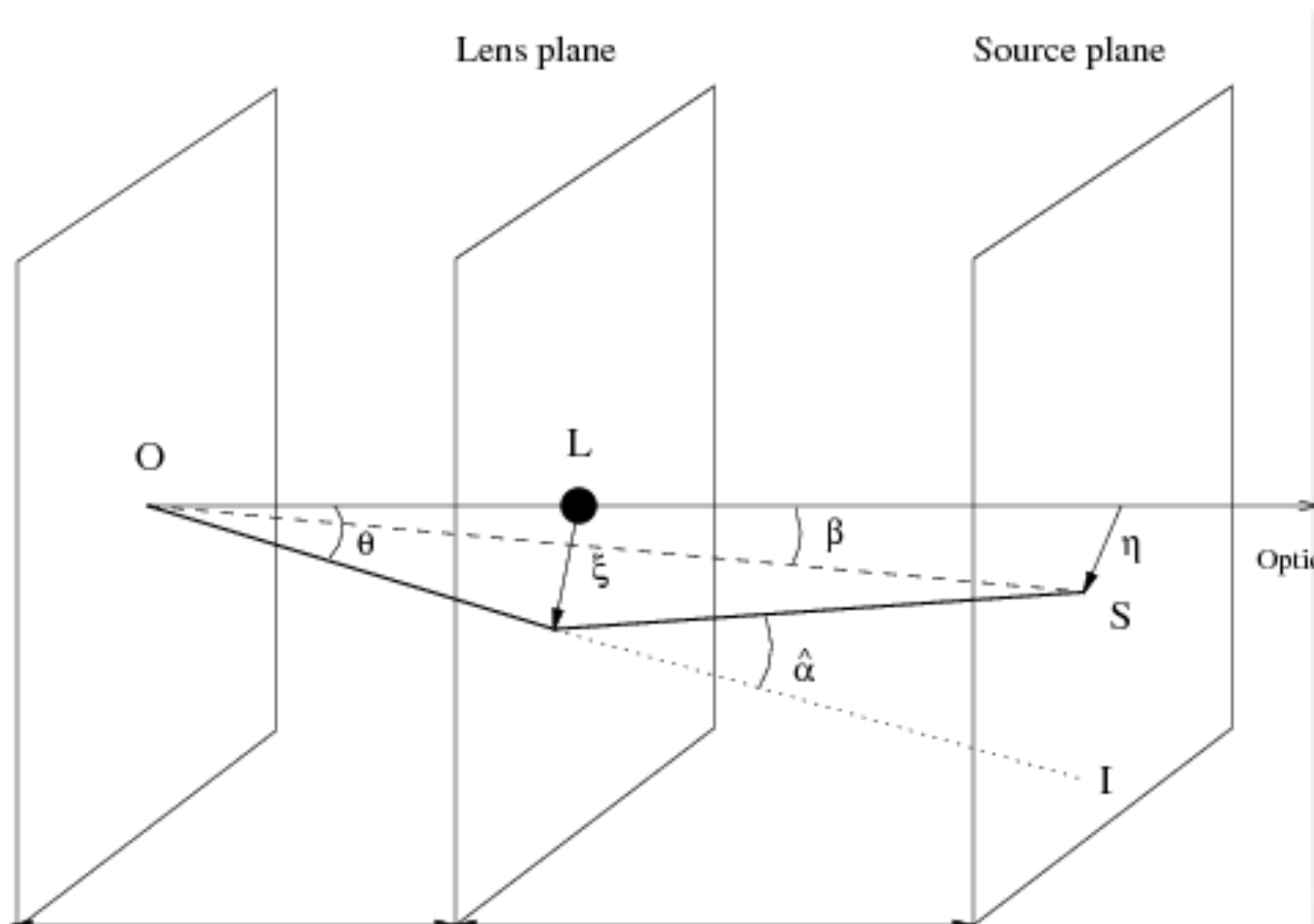
By varying the parameter used in the parameterisation, one can get a range of qualitatively different behaviours seen in many other models. A representative model that can be a good testbed.

Weak Gravitational Lensing

Weak Gravitational Lensing

- Gravitational lensing describes the effect that light rays (trajectories of photons) are deflected in a gravitational field.
- In strong gravitational field, the effect is known as strong lensing, e.g., Einstein rings.
- We will focus on the weak gravitational lensing effect, which is the deflection of light rays by the large scale structure. This will cause slight distortions of the images of distant galaxies, e.g., a round galaxy would appear slightly elliptical.
- However, the effect is so weak that it is dominated by intrinsic ellipticity and random orientations of galaxies. Instead, the effect is commonly observed by the averaged effect of many galaxies.

Weak Gravitational Lensing



Picture taken from Umetsu 2010

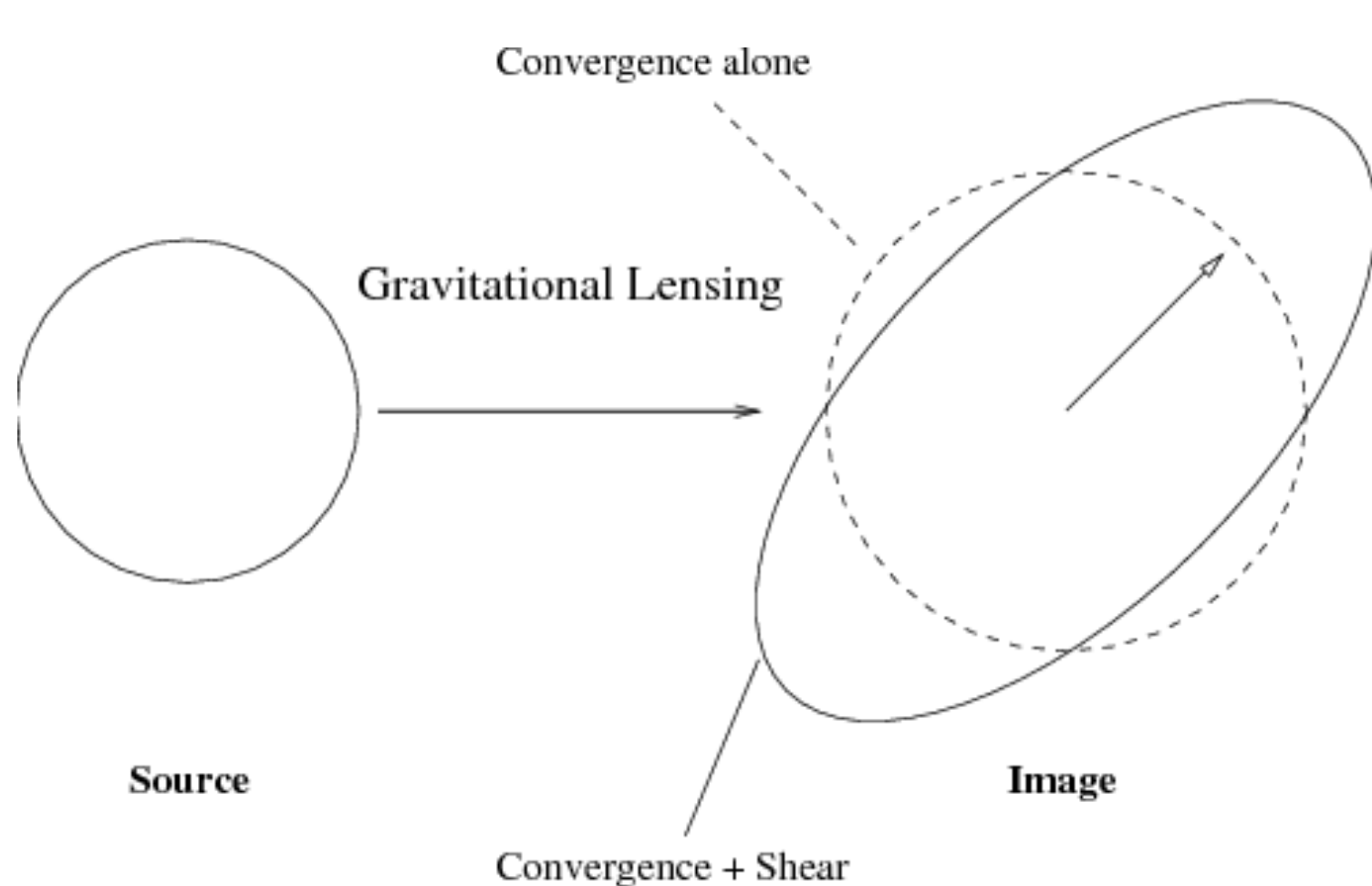
Due to the deflection of light rays, the image of a distant object (source) will appear distorted from its true shape.

The distortion can be described using deformation matrix.

To 1st order, the deformation matrix can be written as:

$$\hat{A} = \begin{bmatrix} 1 - \kappa - \gamma_1 & -\gamma_2 \\ -\gamma_2 & 1 - \kappa + \gamma_1 \end{bmatrix}$$

Weak Gravitational Lensing



κ : convergence, magnification
(change of size)

(γ_1, γ_2) : shear, distortion
(change of shape)

$$\begin{aligned}\kappa &= 1 - (A_1^1 + A_2^2) / 2 \\ &= \frac{1}{c^2} \int_0^{\chi_s} g(\chi_s, \chi) [\nabla^1 \nabla_1 \Phi + \nabla^2 \nabla_2 \Phi] d\chi\end{aligned}$$

$$\hat{A} = \begin{bmatrix} 1 - \kappa - \gamma_1 & -\gamma_2 \\ -\gamma_2 & 1 - \kappa + \gamma_1 \end{bmatrix}$$

Weak Gravitational Lensing

$$\begin{aligned}\kappa &= 1 - (A_1^1 + A_2^2) / 2 \\ &= \frac{1}{c^2} \int_0^{\chi_s} g(\chi_s, \chi) [\nabla^1 \nabla_1 \Phi + \nabla^2 \nabla_2 \Phi] d\chi \\ \gamma_1 &= -(A_1^1 - A_2^2) / 2 \\ &= \frac{1}{c^2} \int_0^{\chi_s} g(\chi_s, \chi) [\nabla^1 \nabla_1 \Phi - \nabla^2 \nabla_2 \Phi] d\chi \\ \gamma_2 &= -A_2^1 = -A_1^2 \\ &= \frac{2}{c^2} \int_0^{\chi_s} g(\chi_s, \chi) \nabla^1 \nabla_2 \Phi d\chi,\end{aligned}$$

κ : convergence, magnification
(change of size)

(γ_1, γ_2) : shear, distortion
(change of shape)

For weak lensing, shear and convergence are directly related, it is often enough to study one.

$$\hat{A} = \begin{bmatrix} 1 - \kappa - \gamma_1 & -\gamma_2 \\ -\gamma_2 & 1 - \kappa + \gamma_1 \end{bmatrix}$$

Weak Lensing Convergence

$$\begin{aligned}\kappa &= 1 - (A_1^1 + A_2^2) / 2 \\ &= \frac{1}{c^2} \int_0^{\chi_s} g(\chi_s, \chi) [\nabla^1 \nabla_1 \Phi + \nabla^2 \nabla_2 \Phi] d\chi\end{aligned}$$

$$\begin{aligned}c^2 \kappa &= \int_0^{\chi_s} g(\chi_s, \chi) [\nabla^2 \Phi - \nabla_\chi^2 \Phi] d\chi \\ &= \left[\frac{3}{2} \Omega_{m0} H_0^2 \int_0^{\chi_s} g(\chi_s, \chi) \frac{\delta}{a} d\chi \right] + \int_0^{\chi_s} \nabla_\chi \Phi \partial_\chi g d\chi + \frac{1}{c} \int_0^{\chi_s} g \partial_t (\nabla_\chi \Phi) d\chi - g \nabla_\chi \Phi \Big|_0^{\chi_s}\end{aligned}$$

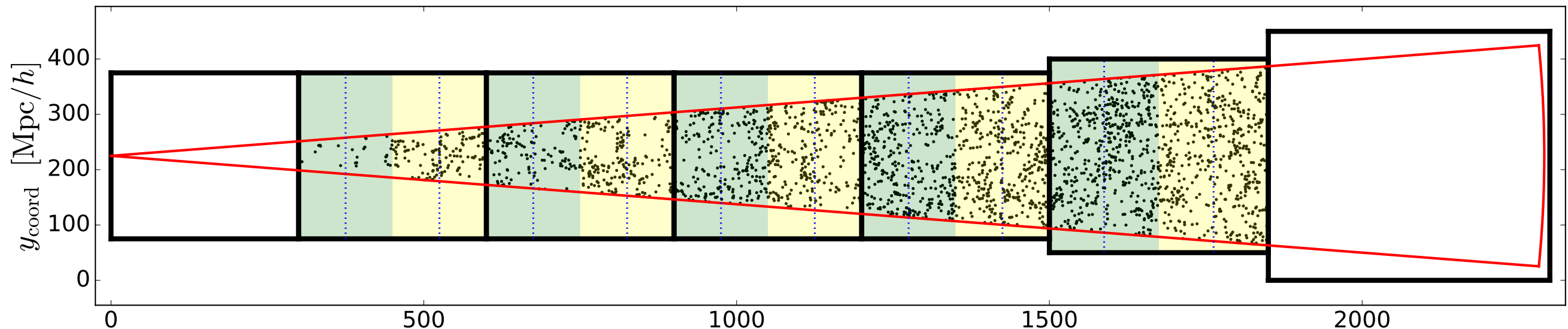
Weak Lensing Convergence

$$\begin{aligned}\kappa &= 1 - (A_1^1 + A_2^2) / 2 \\ &= \frac{1}{c^2} \int_0^{\chi_s} g(\chi_s, \chi) [\nabla^1 \nabla_1 \Phi + \nabla^2 \nabla_2 \Phi] d\chi\end{aligned}$$

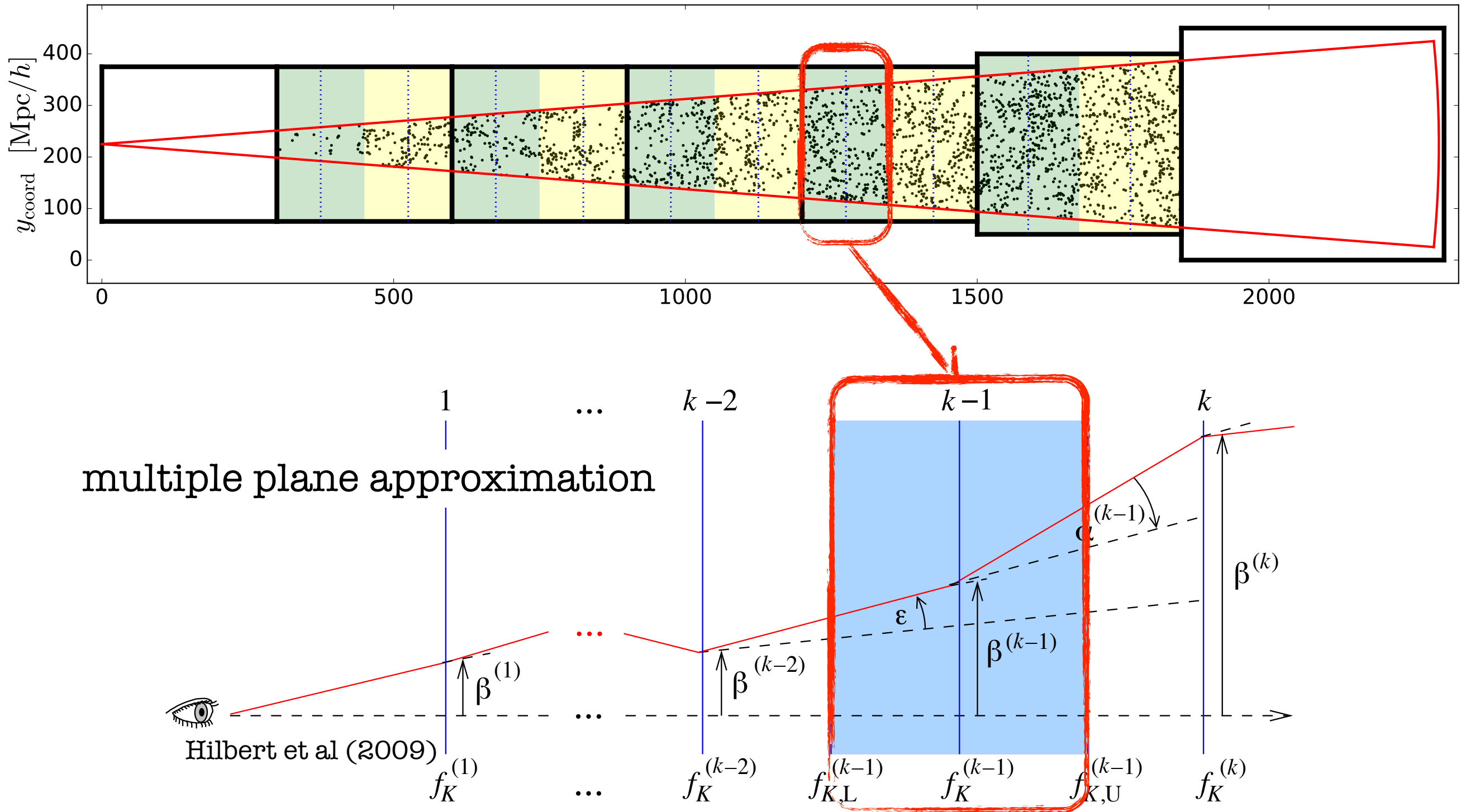
$$\begin{aligned}c^2 \kappa &= \int_0^{\chi_s} g(\chi_s, \chi) [\nabla^2 \Phi - \nabla_\chi^2 \Phi] d\chi \\ &= \left[\frac{3}{2} \Omega_{m0} H_0^2 \int_0^{\chi_s} g(\chi_s, \chi) \frac{\delta}{a} d\chi \right] + \int_0^{\chi_s} \nabla_\chi \Phi \partial_\chi g d\chi + \frac{1}{c} \int_0^{\chi_s} g \partial_t (\nabla_\chi \Phi) d\chi - g \nabla_\chi \Phi \Big|_0^{\chi_s}\end{aligned}$$

This becomes a weighted integration of the matter density field along the line of sight

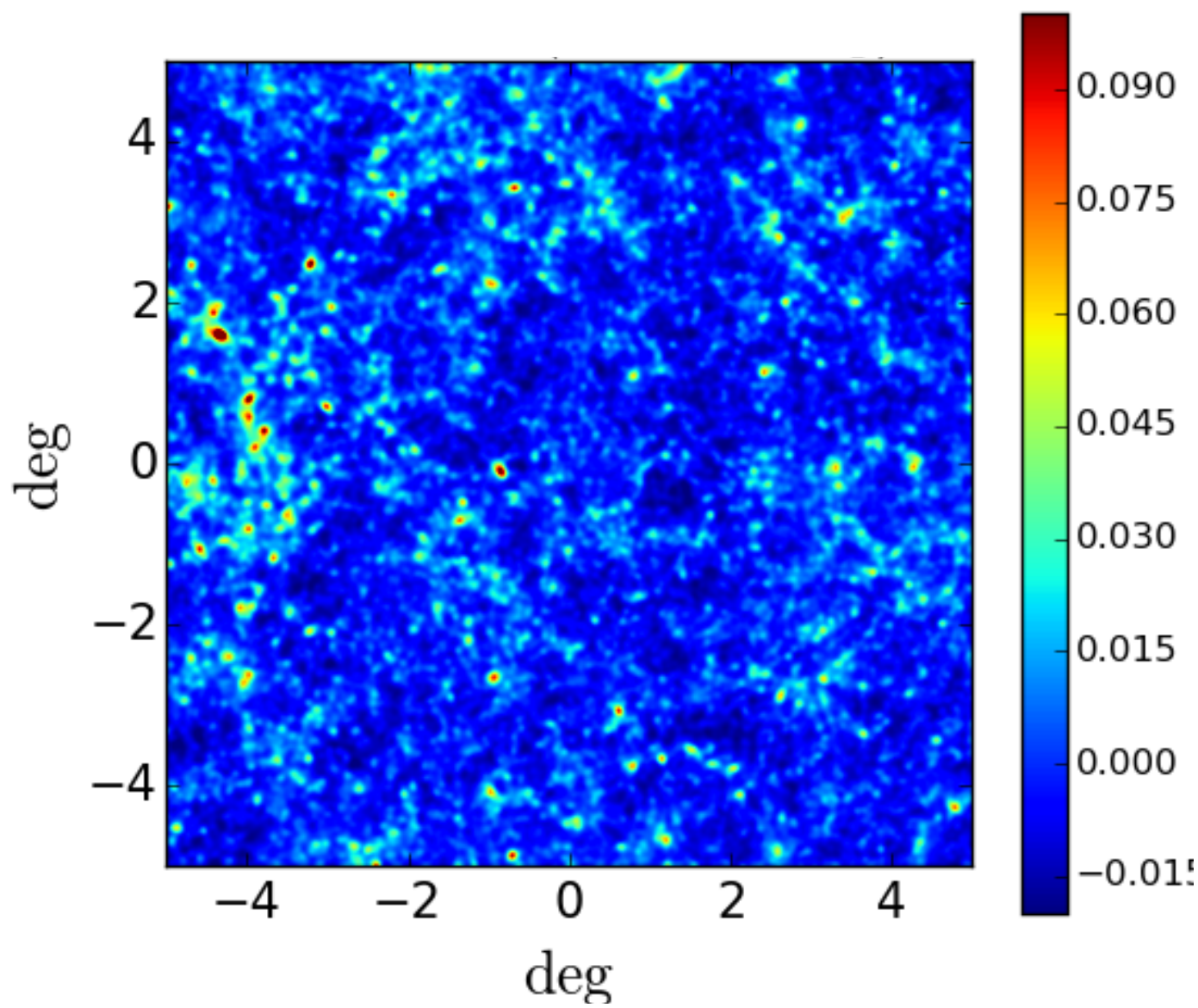
Ray Tracing Simulations



Ray Tracing Simulations



Weak Lensing Convergence Maps

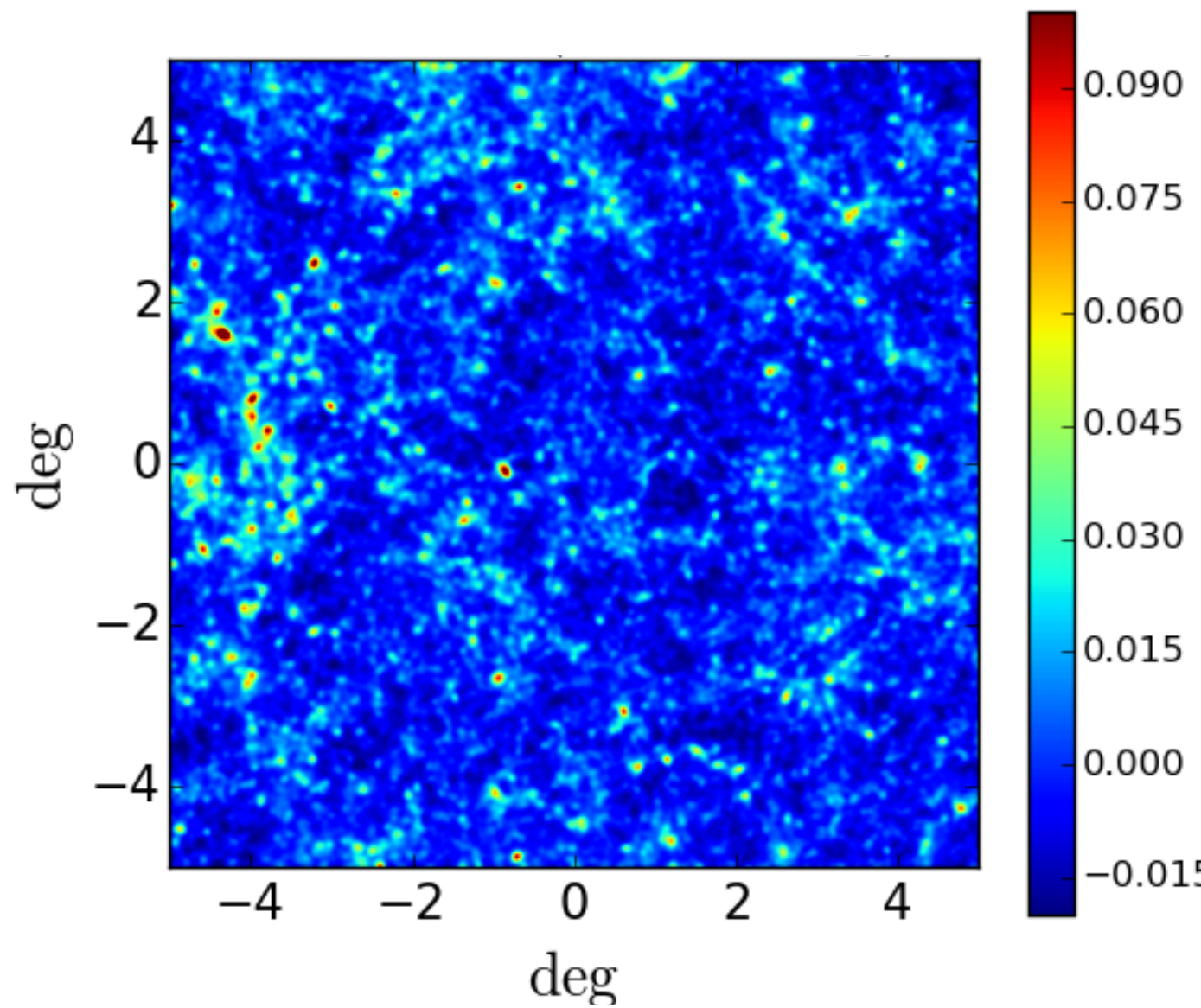


These are 2D maps whose information can be obtained statistically.

The results can be compared to similar statistical quantities from the observed lensing (shear) map, to tell us information about cosmological parameters and cosmological models.

rich info; potential good tests

Weak Lensing Convergence Maps



Some common examples:

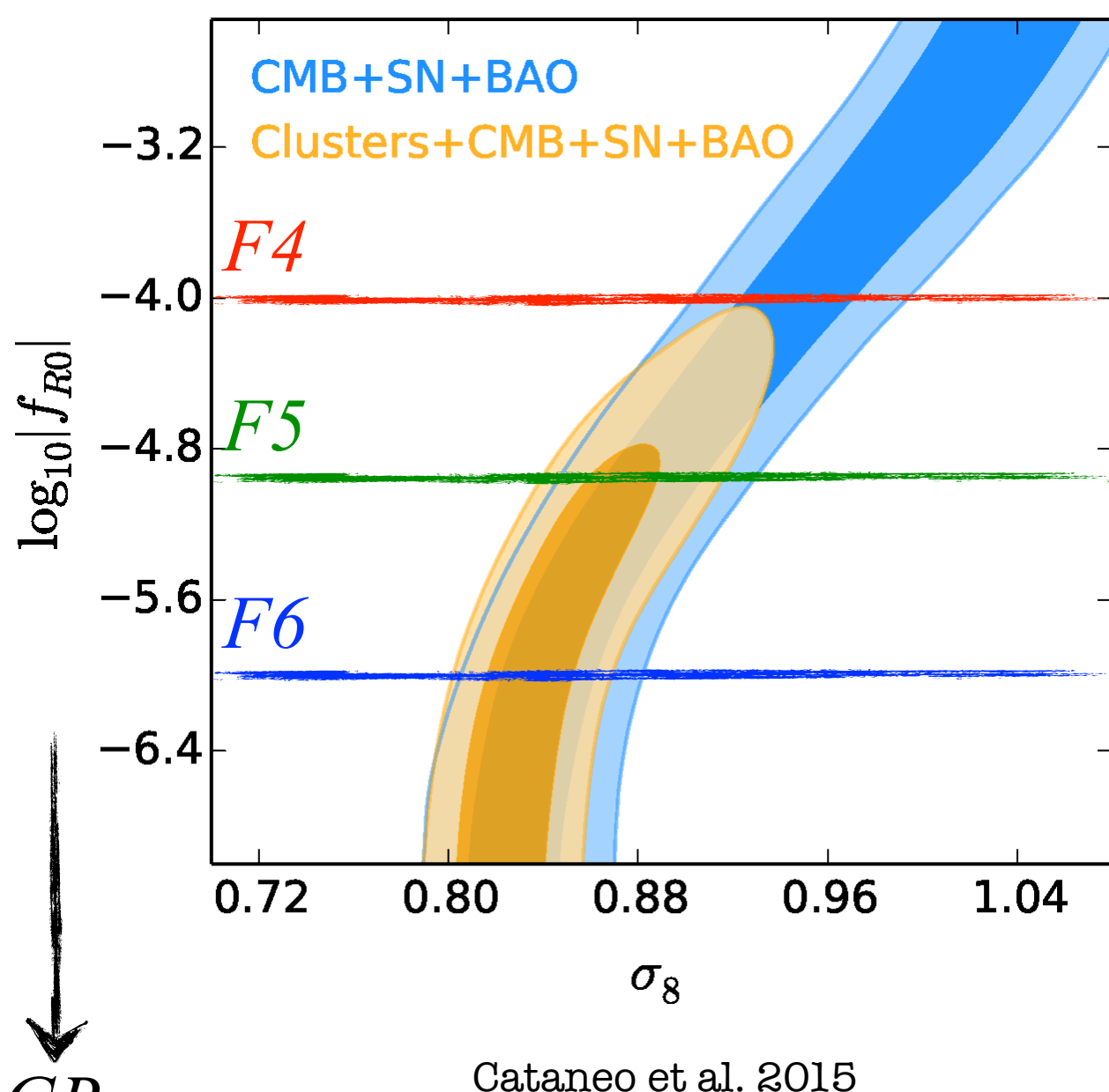
1-point statistic: peak counts

2-point statistic: 2-point correlation function (in real space) and angular power spectrum (in Fourier space)

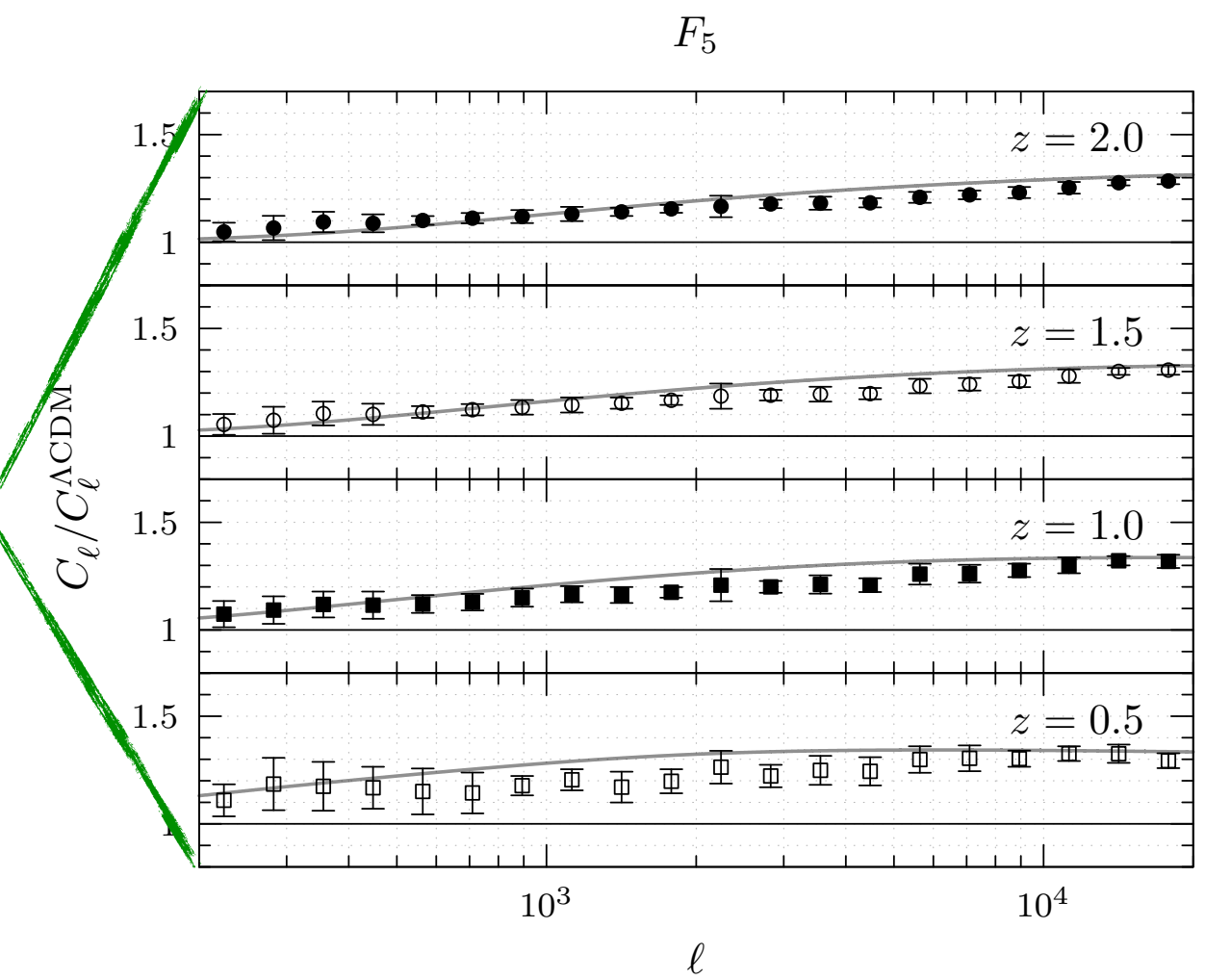
n-point statistics: non-Gaussianity

morphological statistics: Minkowski functionals

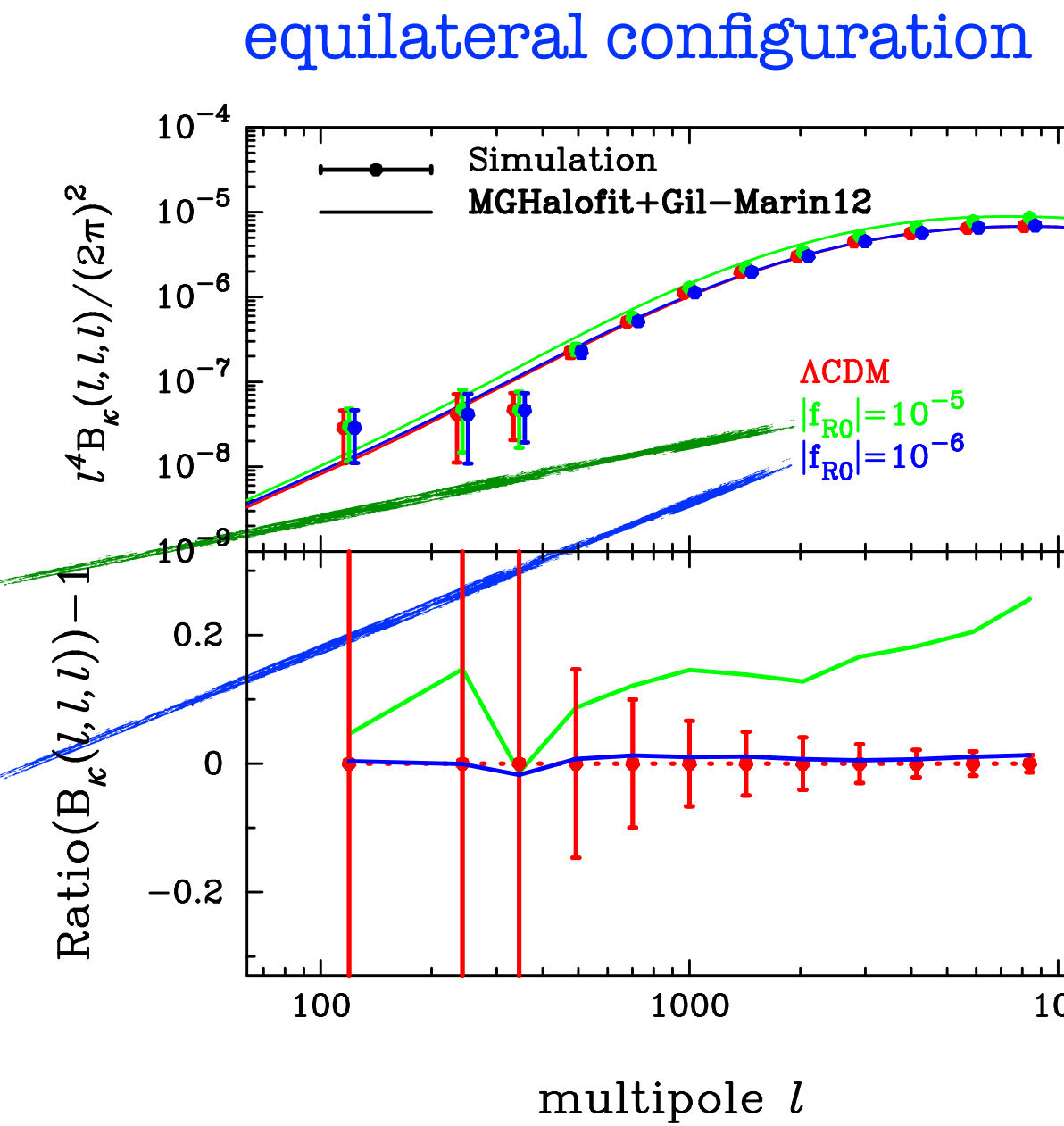
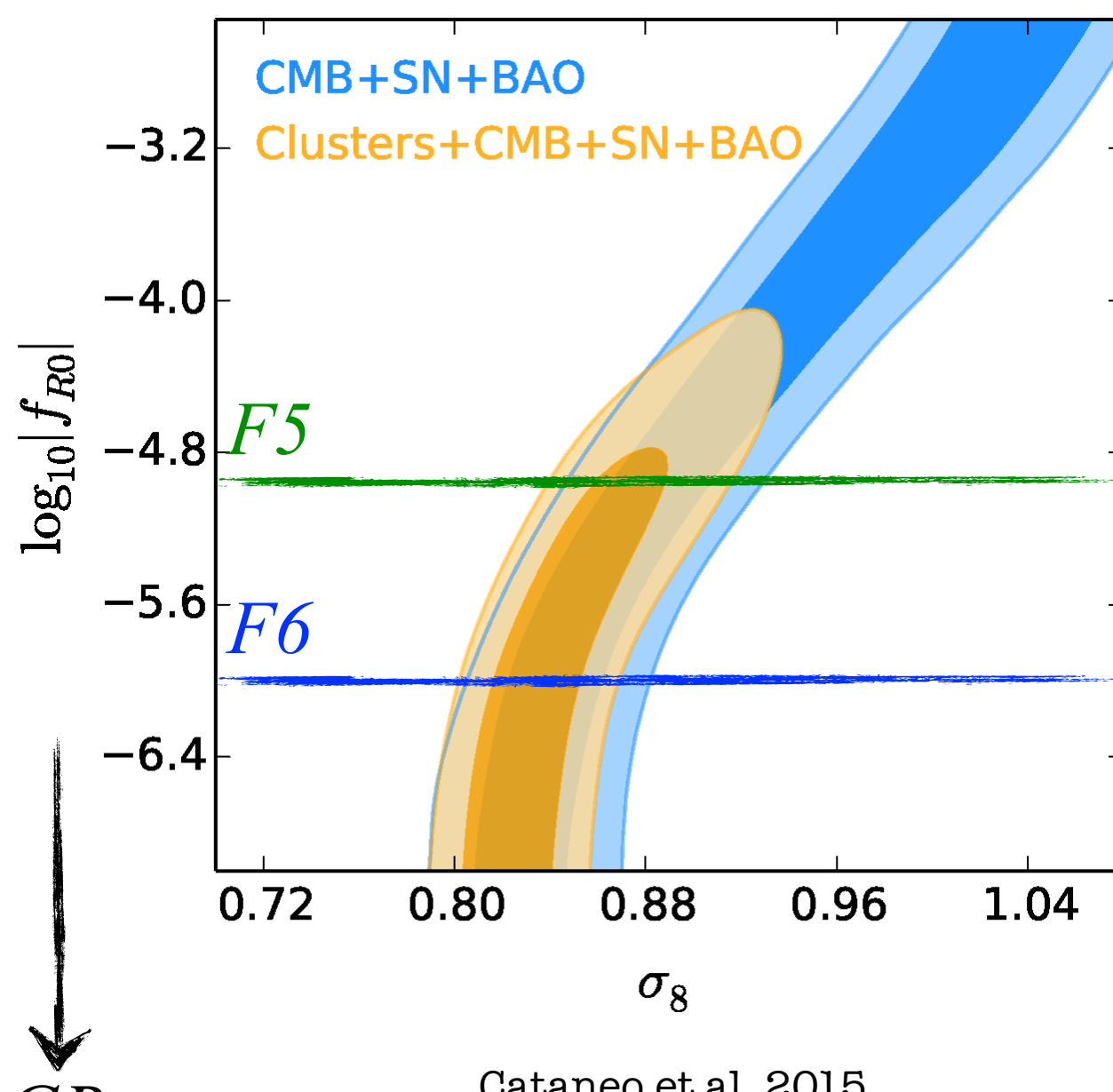
Example I: Convergence Power Spectrum



WL convergence PS



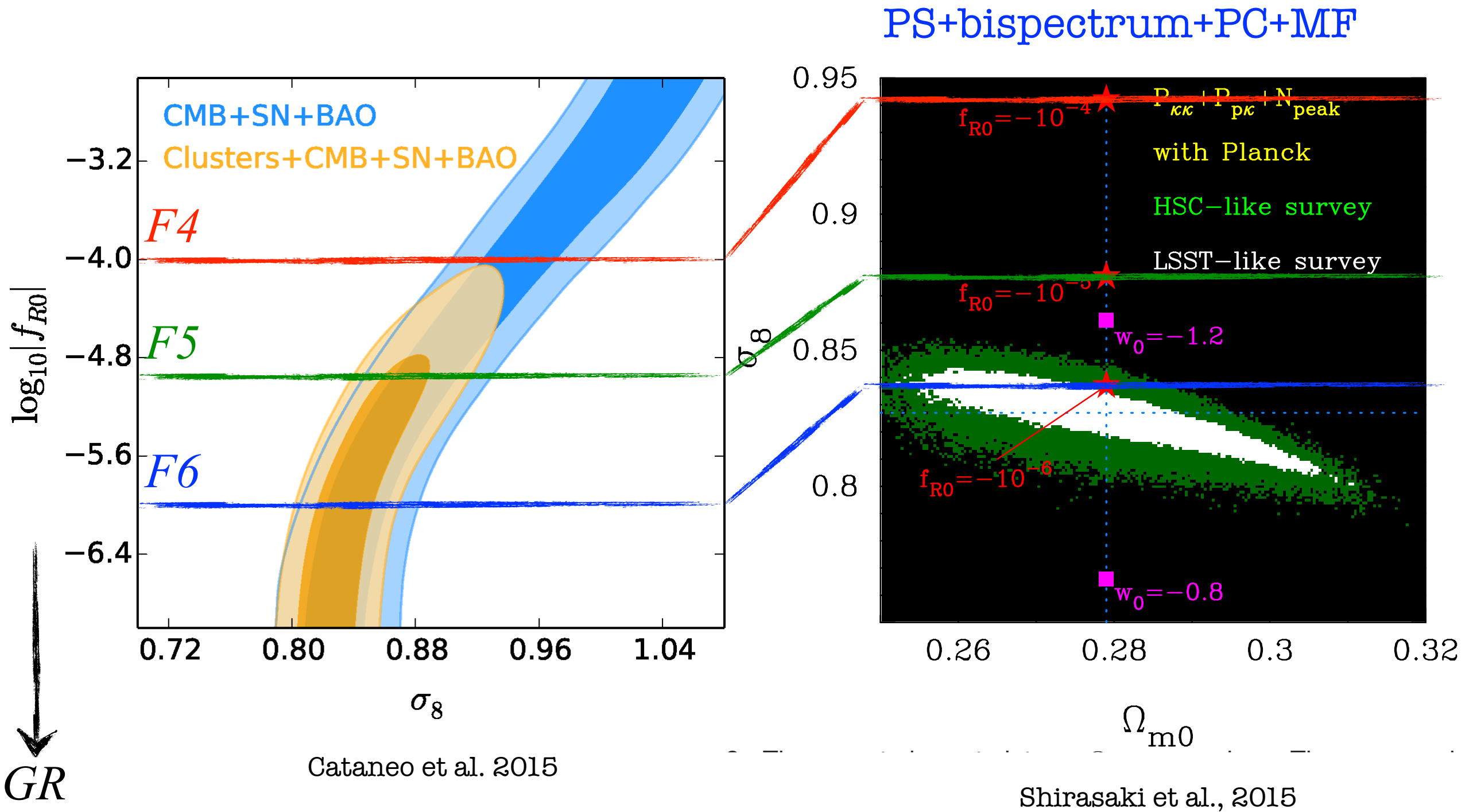
Example 2: Convergence Bipectrum



\downarrow
 GR

Shirasaki et al., in prep.

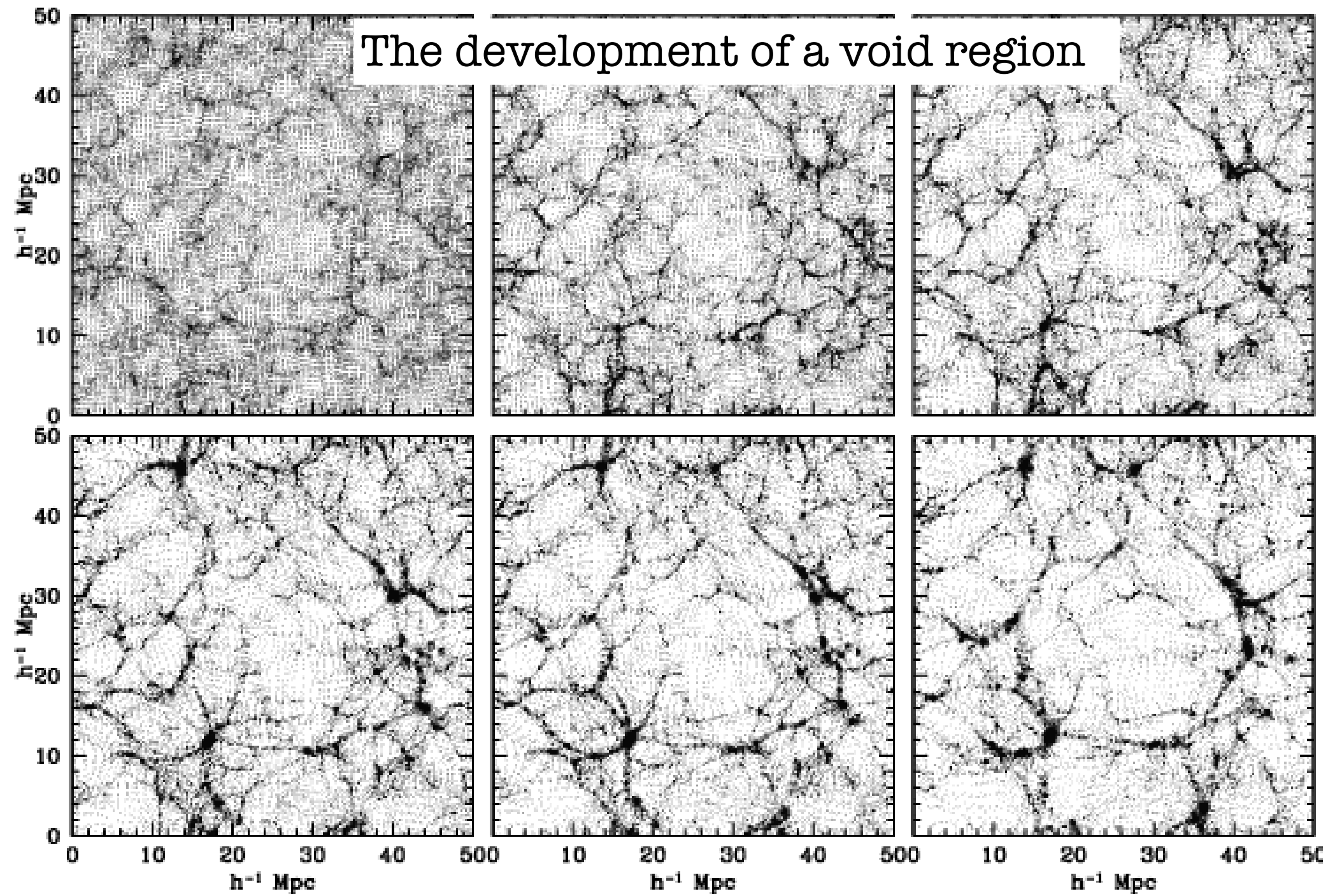
Example 3: Combined



Baryonic effect

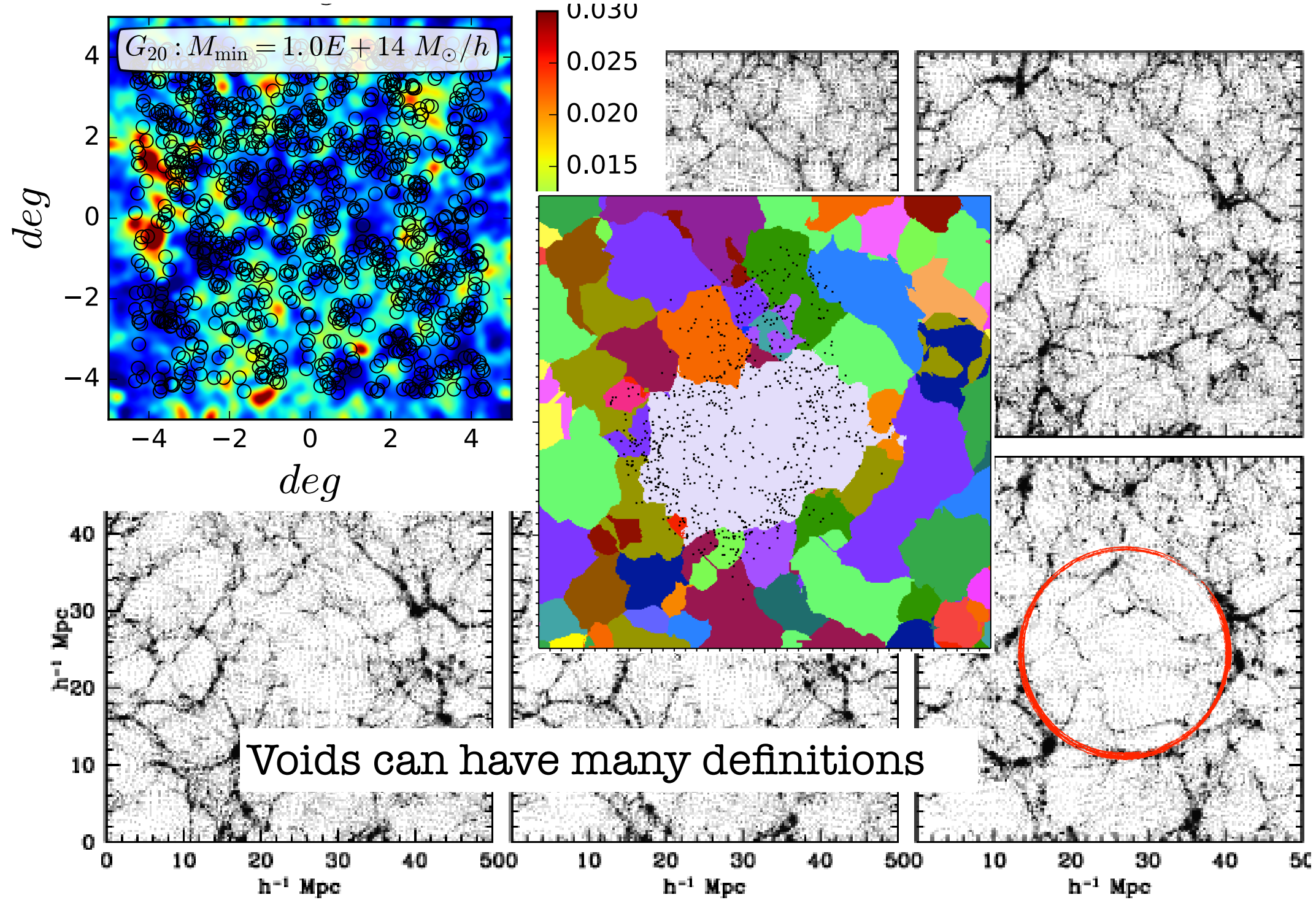
- One advantage of gravitational lensing is that (at least in standard gravity) baryonic matter and dark matter deflect the photon trajectories in the same way
- As a result, weak lensing directly probes total matter
- However, various baryonic processes can still have an impact on the matter distribution on small scales. For example, AGN feedback could change the density profile of clusters, therefore affecting lensing result.
- It is difficult enough to model in LCDM, more so for nonstandard models. For this reason, one should perhaps avoid using small scale data to make definite conclusions.

Weak Lensing by Voids



Sheth & van de Weygaert 2004

Weak Lensing by Voids

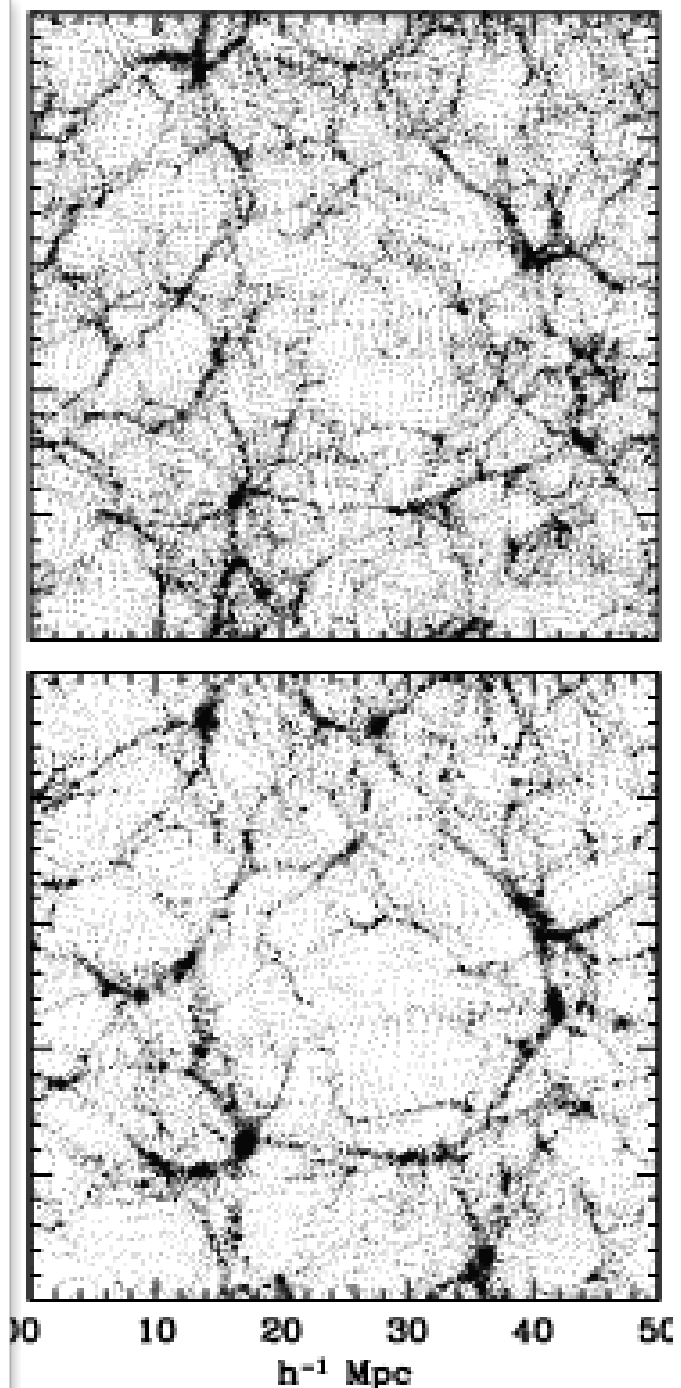


Weak Lensing by Voids

Like any other structure in the Universe (e.g., clusters), voids can cause deflection of light rays and (anti)lensing

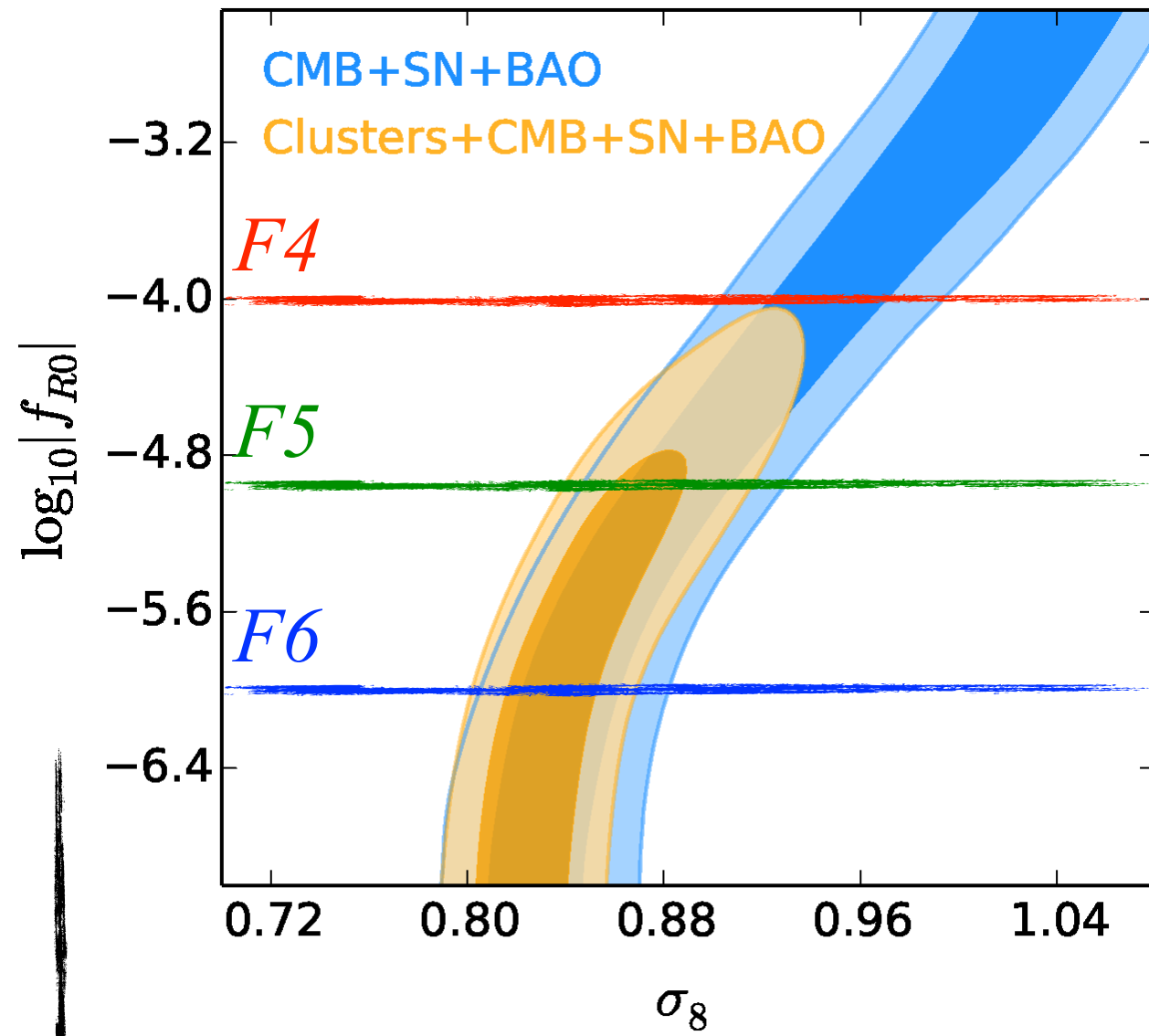
But there are difficulties in using void lensing:

1. voids do not have a common definition; has to try different definitions to find the optimal one
2. voids have very low density contrast and noisy density profiles; to study their lensing effect one needs to stack a lot

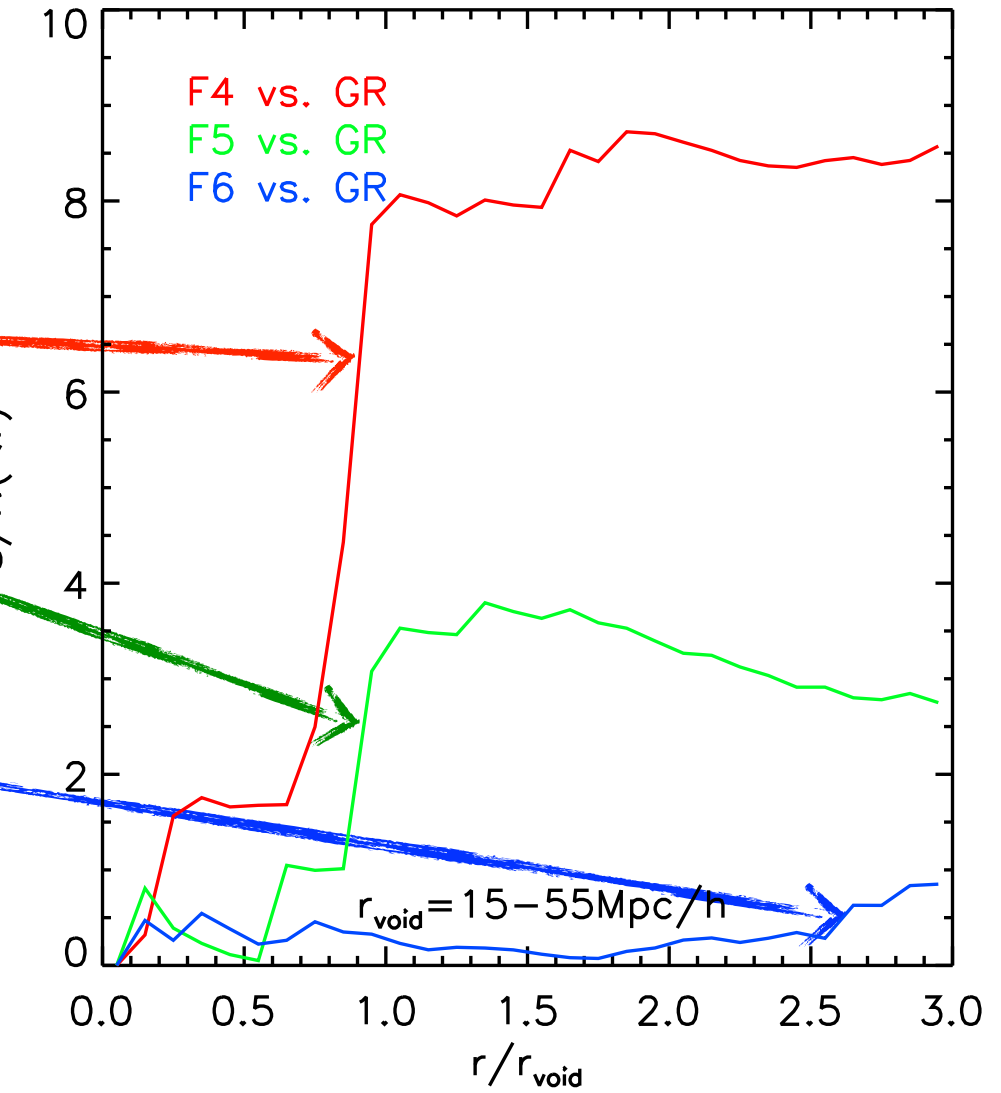


Weak Lensing by Voids

lensing by (stacked) voids



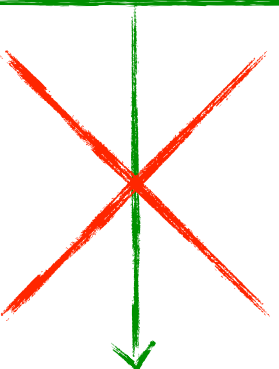
Cataneo et al. 2015



Cai et al., 2015

Ray Shooting Simulations

$$\begin{aligned}\kappa &= 1 - (A_1^1 + A_2^2) / 2 \\ &= \frac{1}{c^2} \int_0^{\chi_s} g(\chi_s, \chi) [\nabla^1 \nabla_1 \Phi + \nabla^2 \nabla_2 \Phi] d\chi\end{aligned}$$



$$\begin{aligned}c^2 \kappa &= \int_0^{\chi_s} g(\chi_s, \chi) [\nabla^2 \Phi - \nabla_\chi^2 \Phi] d\chi \\ &= \left[\frac{3}{2} \Omega_{m0} H_0^2 \int_0^{\chi_s} g(\chi_s, \chi) \frac{\delta}{a} d\chi \right] + \int_0^{\chi_s} \nabla_\chi \Phi \partial_\chi g d\chi\end{aligned}$$

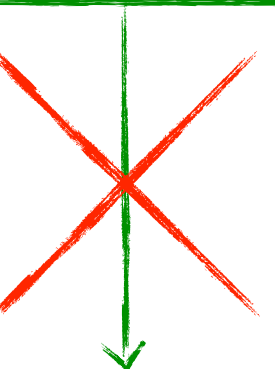
In nonstandard models, the Poisson equation may be modified, so that the above derivation can fail.

One cannot simply project the density field but has to use the full information of the potential.

But one rarely stores the information of the potential (it may not even exist in particle simulations).

Ray Shooting Simulations

$$\begin{aligned}\kappa &= 1 - (A_1^1 + A_2^2) / 2 \\ &= \frac{1}{c^2} \int_0^{\chi_s} g(\chi_s, \chi) [\nabla^1 \nabla_1 \Phi + \nabla^2 \nabla_2 \Phi] d\chi\end{aligned}$$



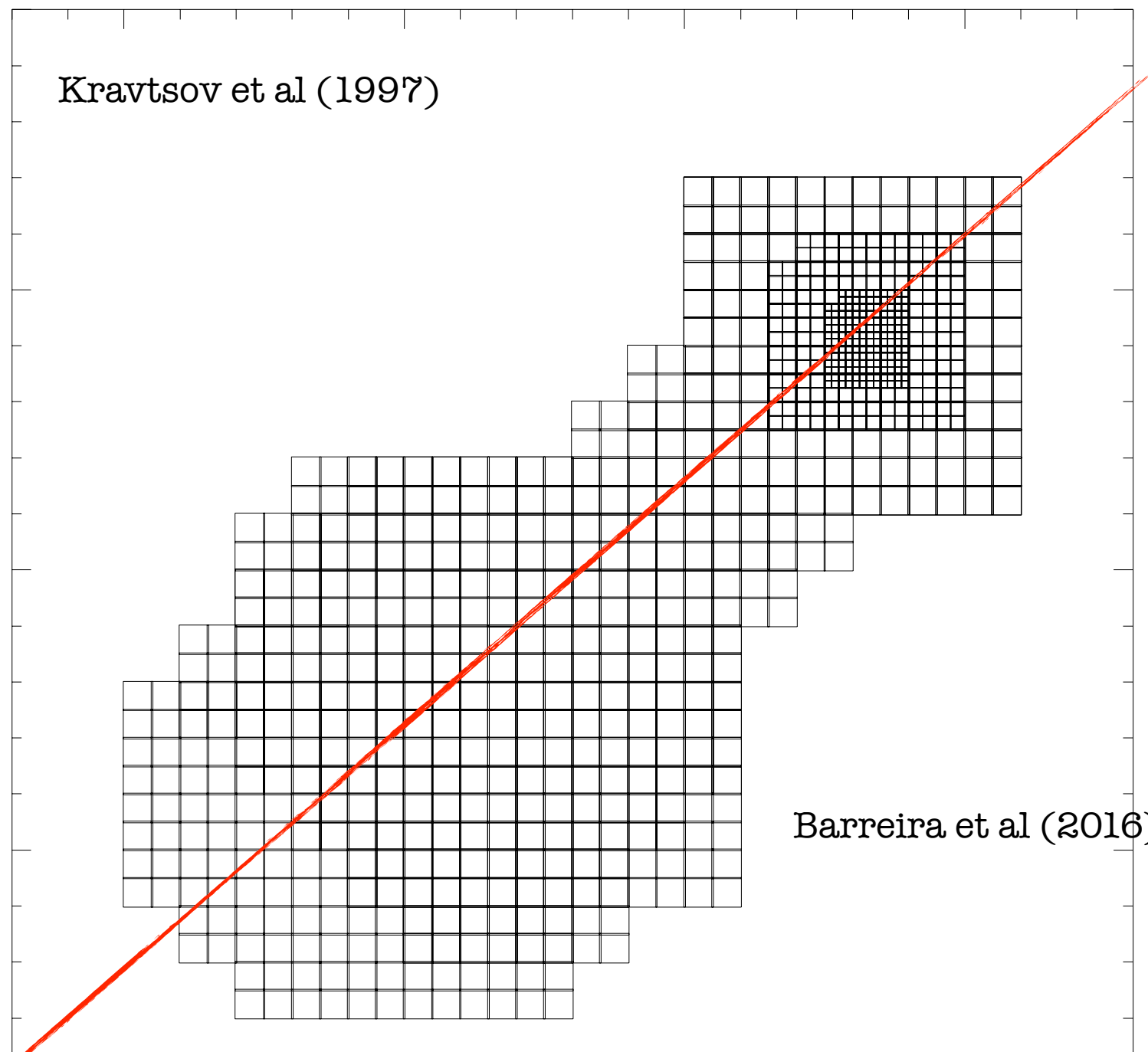
$$\begin{aligned}c^2 \kappa &= \int_0^{\chi_s} g(\chi_s, \chi) [\nabla^2 \Phi - \nabla_\chi^2 \Phi] d\chi \\ &= \left[\frac{3}{2} \Omega_{m0} H_0^2 \int_0^{\chi_s} g(\chi_s, \chi) \frac{\delta}{a} d\chi \right] + \int_0^{\chi_s} \nabla_\chi \Phi \partial_\chi g d\chi\end{aligned}$$

However, in mesh based simulations we generally have very complete information of the potential itself. Can we make use this information?

We can store this information like particle data.

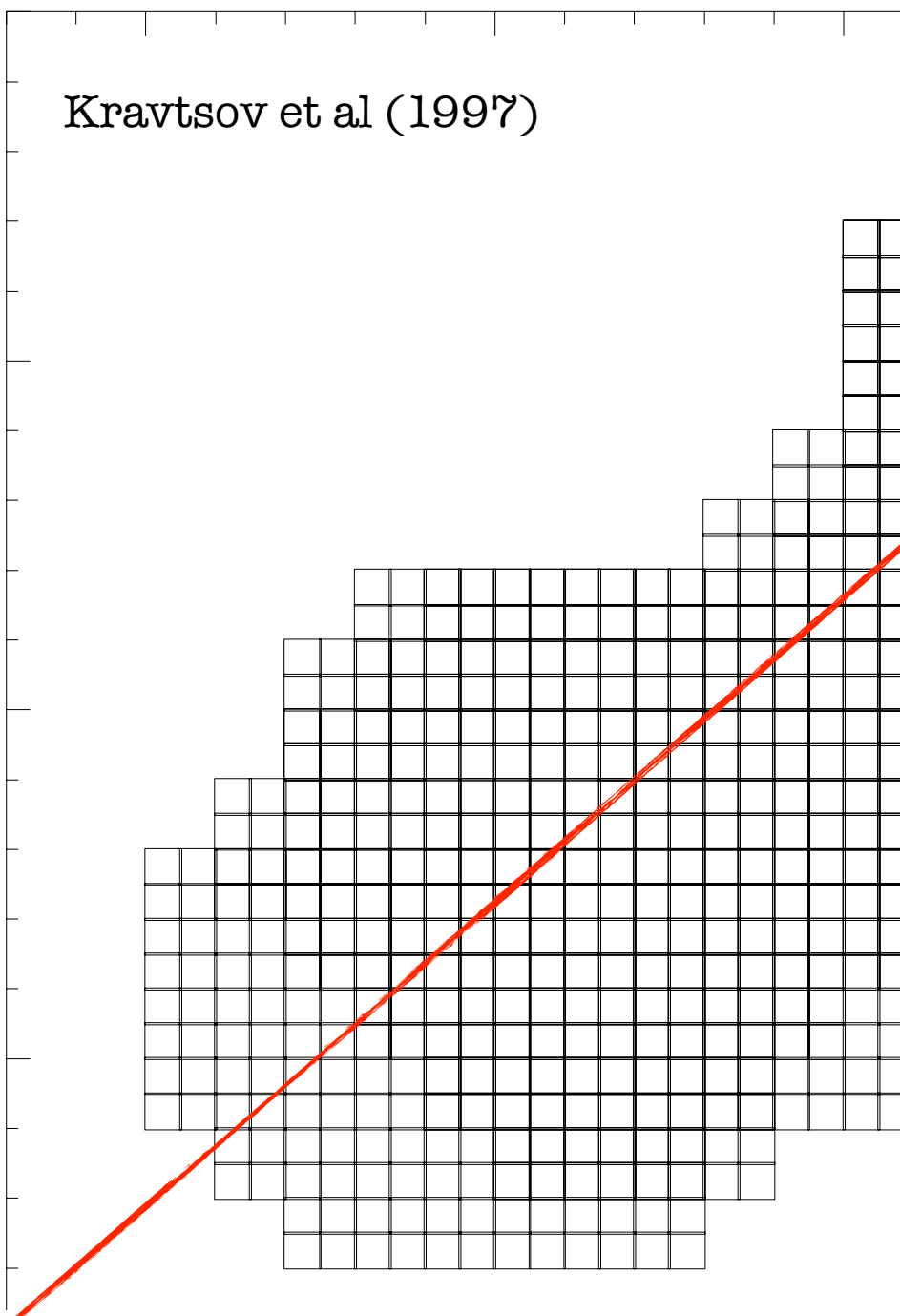
Alternatively, we can do ray tracing on the fly of the simulation when such info is still there

Ray Shooting Simulations



Instead of projecting the density field, project the derivatives of the potential itself. One can do this as the light ray passes each cell.

Ray Shooting Simulations



Pros: accurate analytical integration algorithm available; no need to store loads of info (especially on refinements); straightforward

Cons: has to set up the ray directions before the simulation starts, so that rays arrive at observer today. Ray shooting rather than ray tracing - does not allow non straight rays, but perhaps not a big problem.

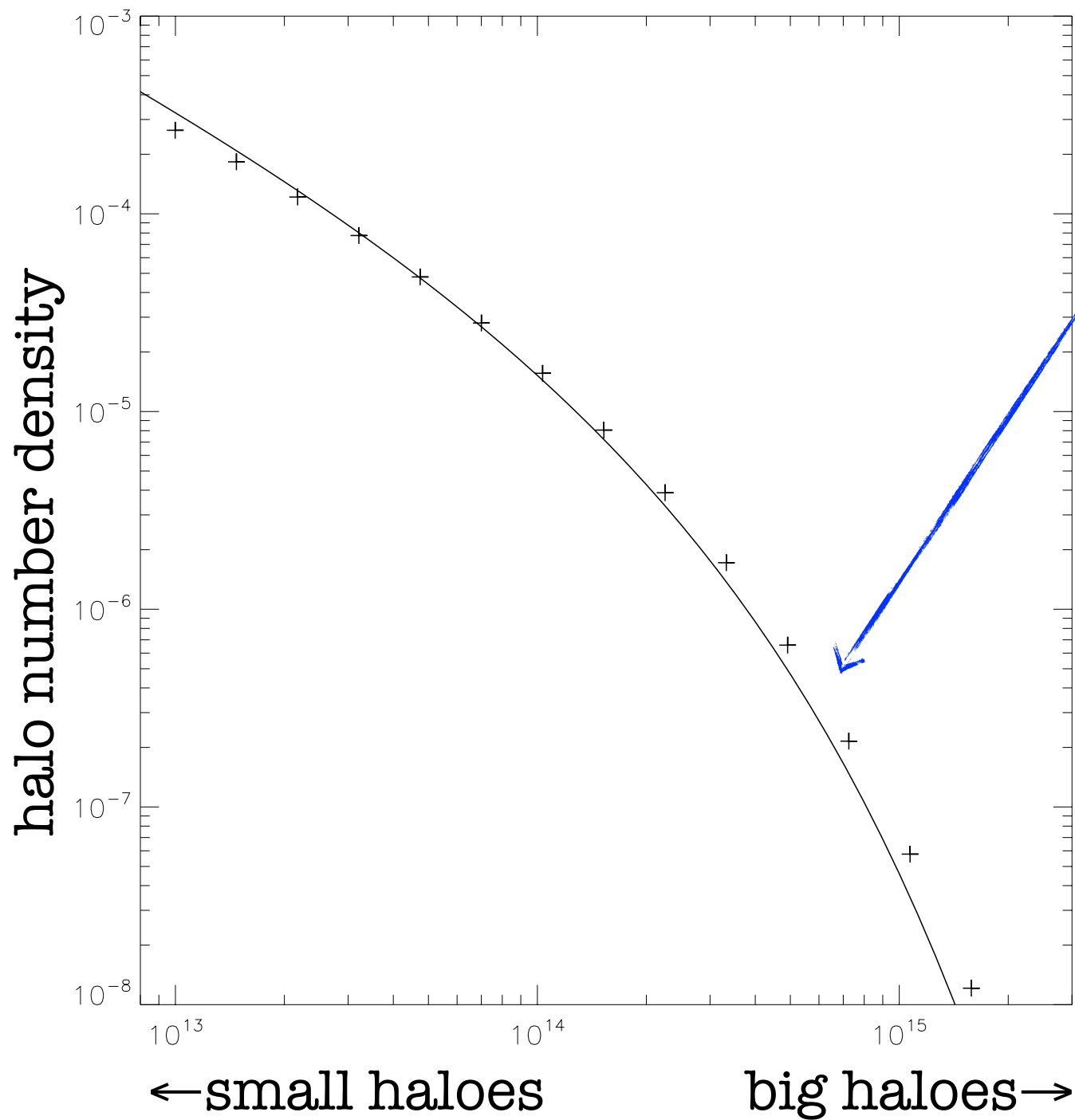
Instead of projecting the density field, project the derivatives of the potential itself. One can do this as the light ray passes each cell.

Clusters of Galaxies

Clusters of Galaxies

- Galaxy clusters are amongst the largest virialised objects in the Universe
- Massive clusters are the real-world counterparts of the dark matter haloes towards the high mass end of the halo mass function
- High mass haloes are rare.

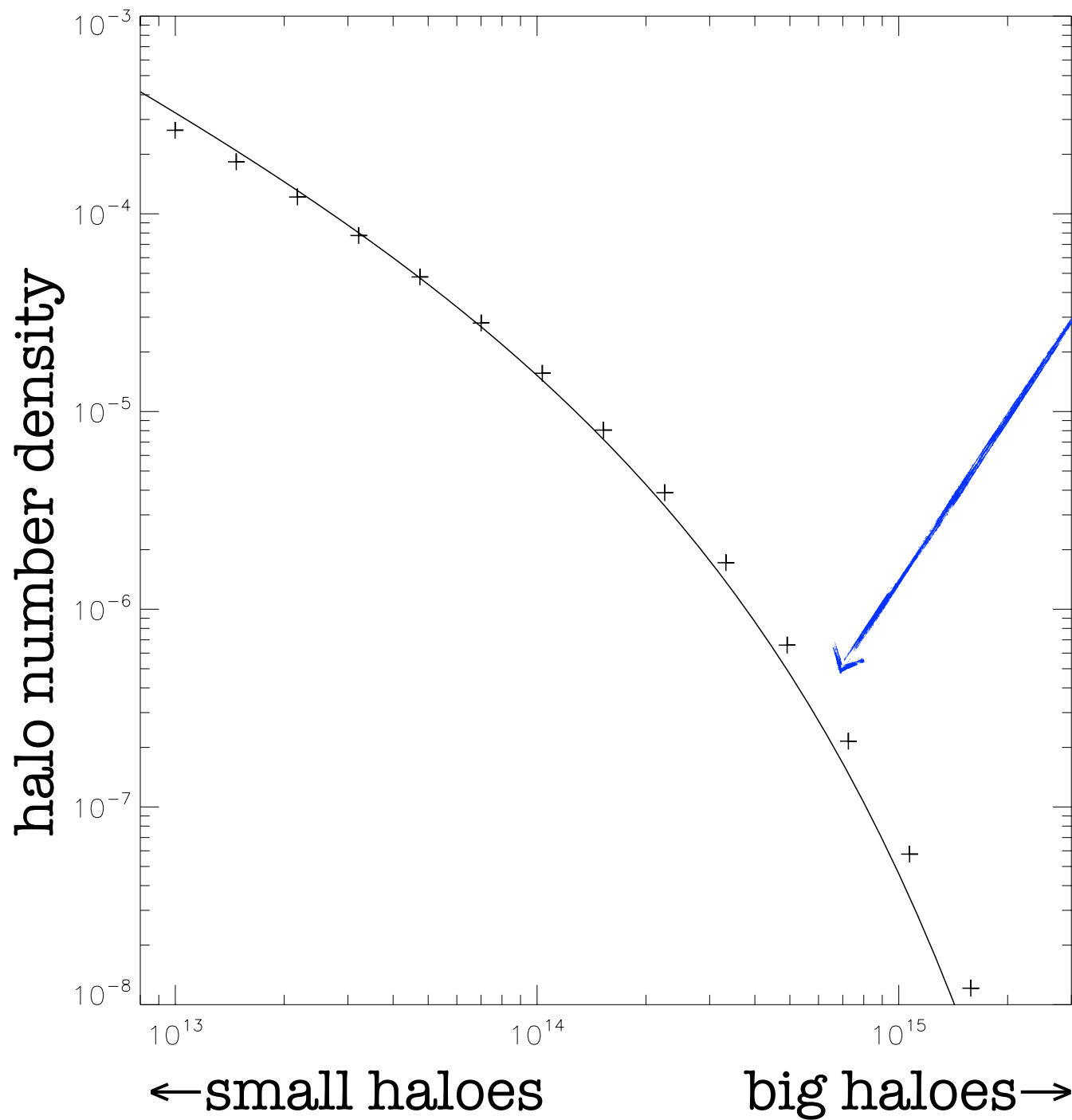
Clusters of Galaxies



There are few massive haloes. The halo mass function becomes very steep towards the high mass end.

Good news: their abundance is sensitive to the expansion rate of the Universe, as well as the nature of gravity, making them an excellent observable to constrain LCDM and test nonstandard models

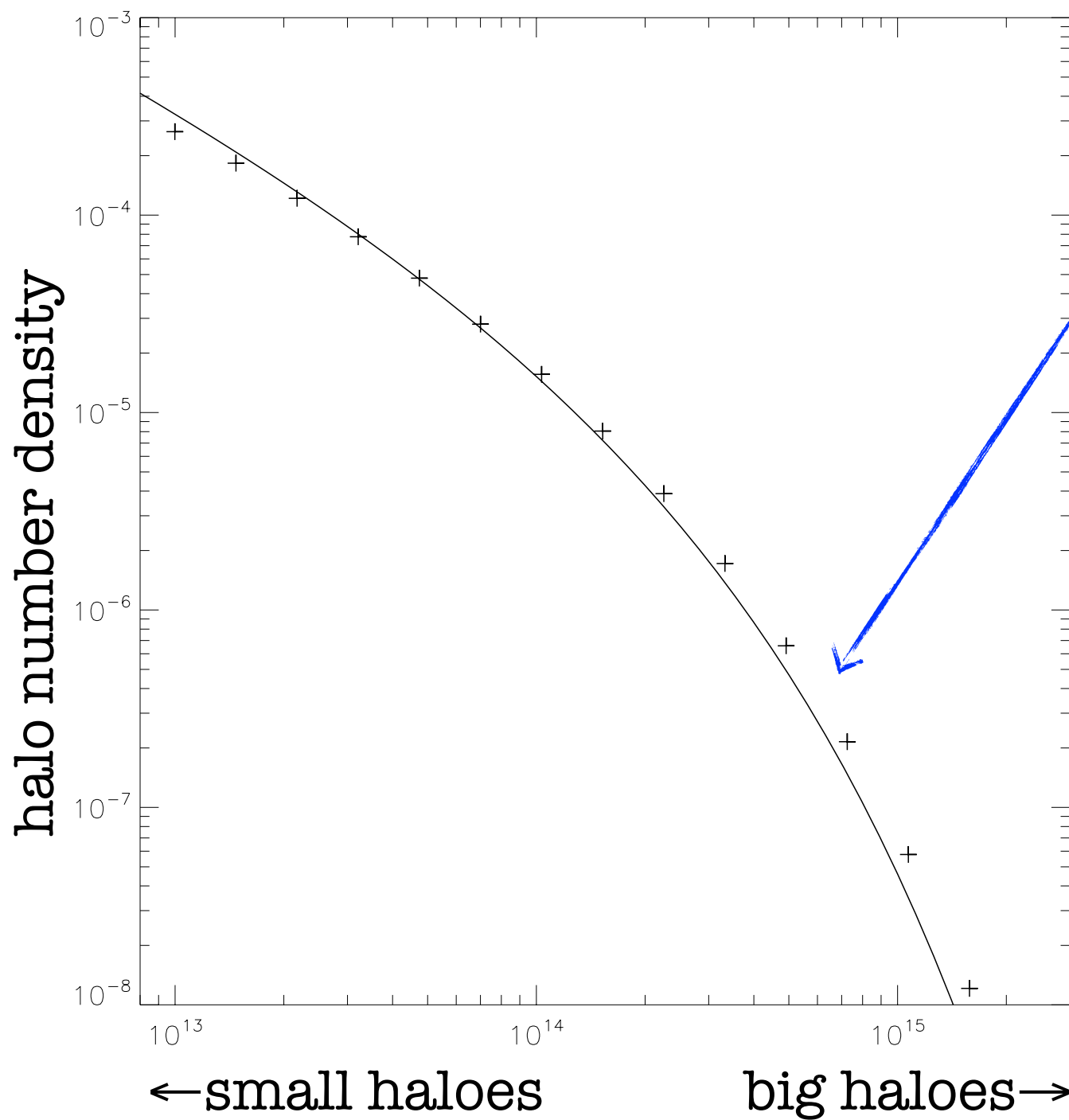
Clusters of Galaxies



There are few massive haloes. The halo mass function becomes very steep towards the high mass end.

Bad news: to use cluster abundance to constrain models, one has to have precise information about cluster mass: a small error can cause a much larger error in abundance.

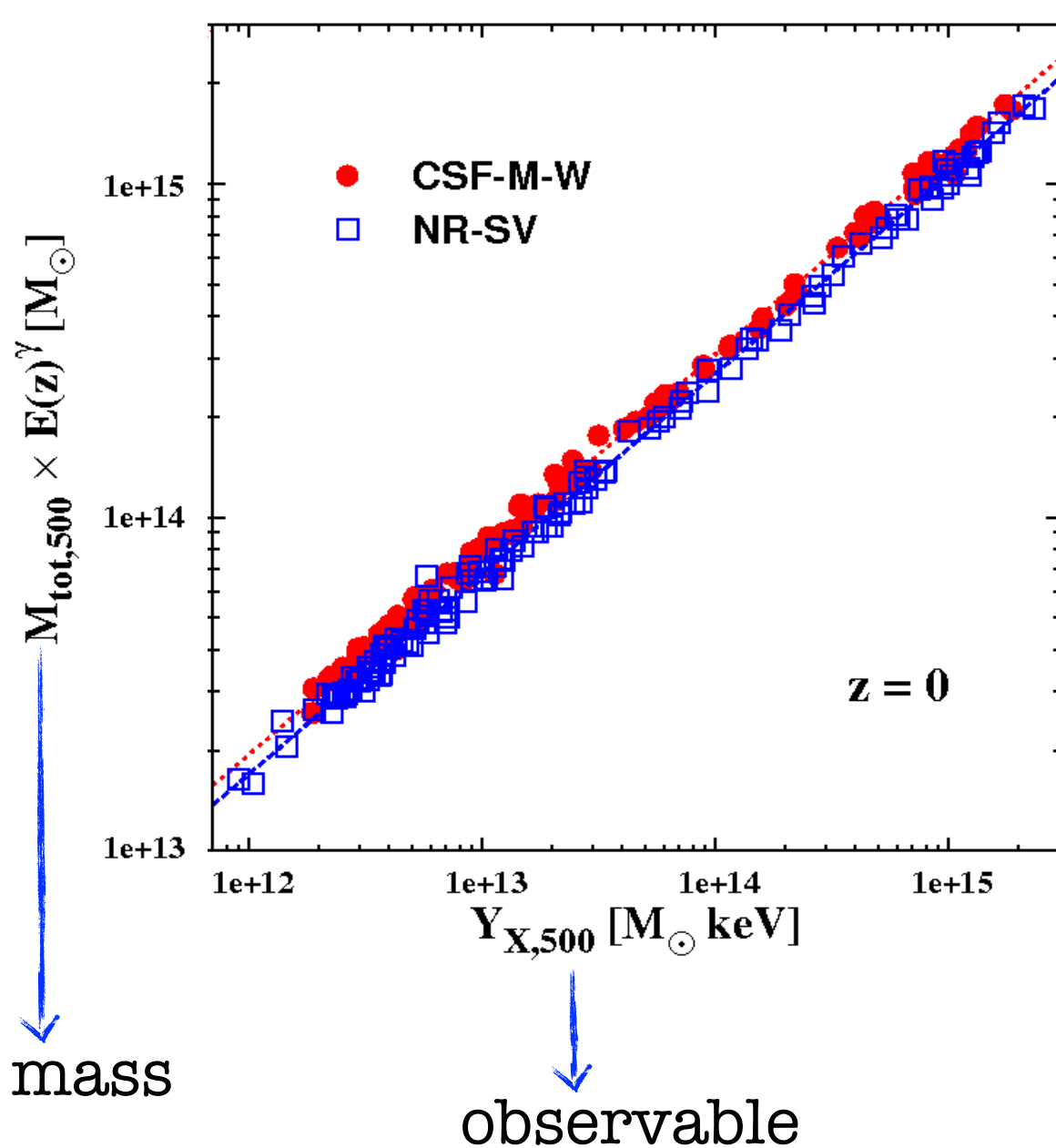
Clusters of Galaxies



There are few massive haloes. The halo mass function becomes very steep towards the high mass end.

Bad news: cluster mass is not a direct observable, but has to be inferred from other observables, e.g., strength of lensing signal, X-ray temperature of cluster, etc.. Intrinsic systematic errors with these observables.

Observable Mass Relations

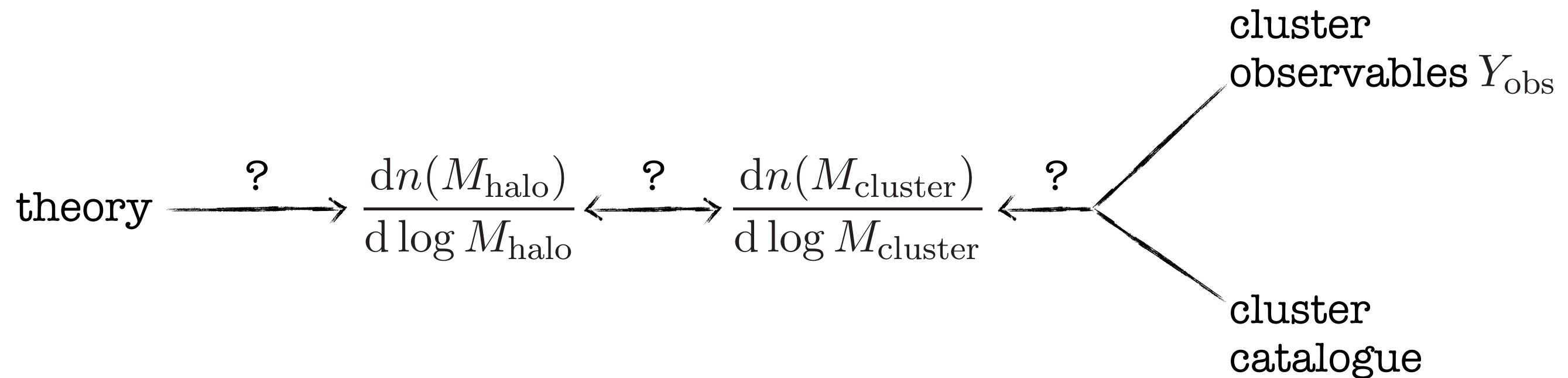


Observable mass relations relate cluster mass with direct observables such as its X-ray temperature.

These can be obtained by fitting to a subset of good quality observational data, or by using state-of-the-art hydrodynamical simulations, etc..

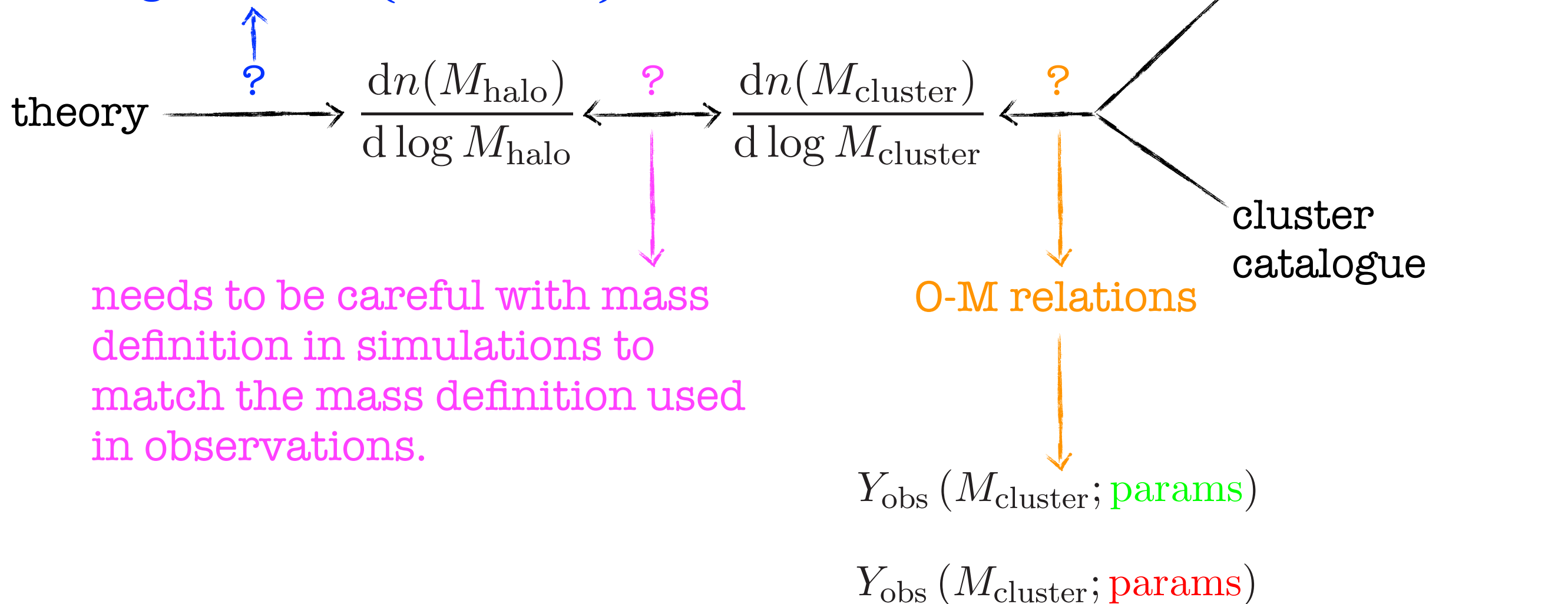
Need parameters to describe the slope and normalisation of the scaling relation.

Testing Models using Cluster Abundance

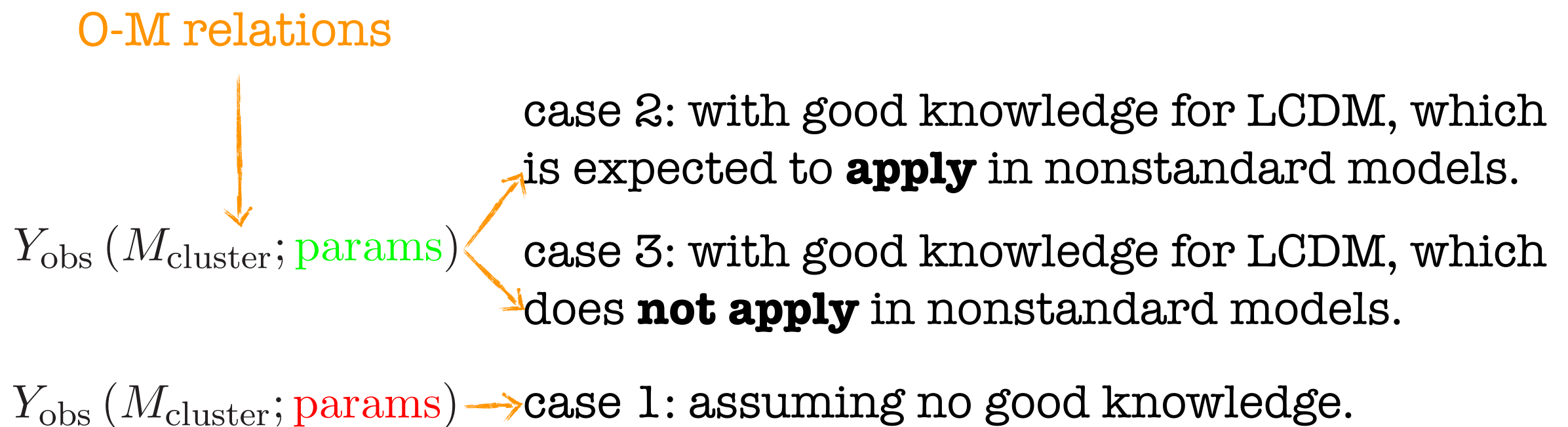


Testing Models using Cluster Abundance

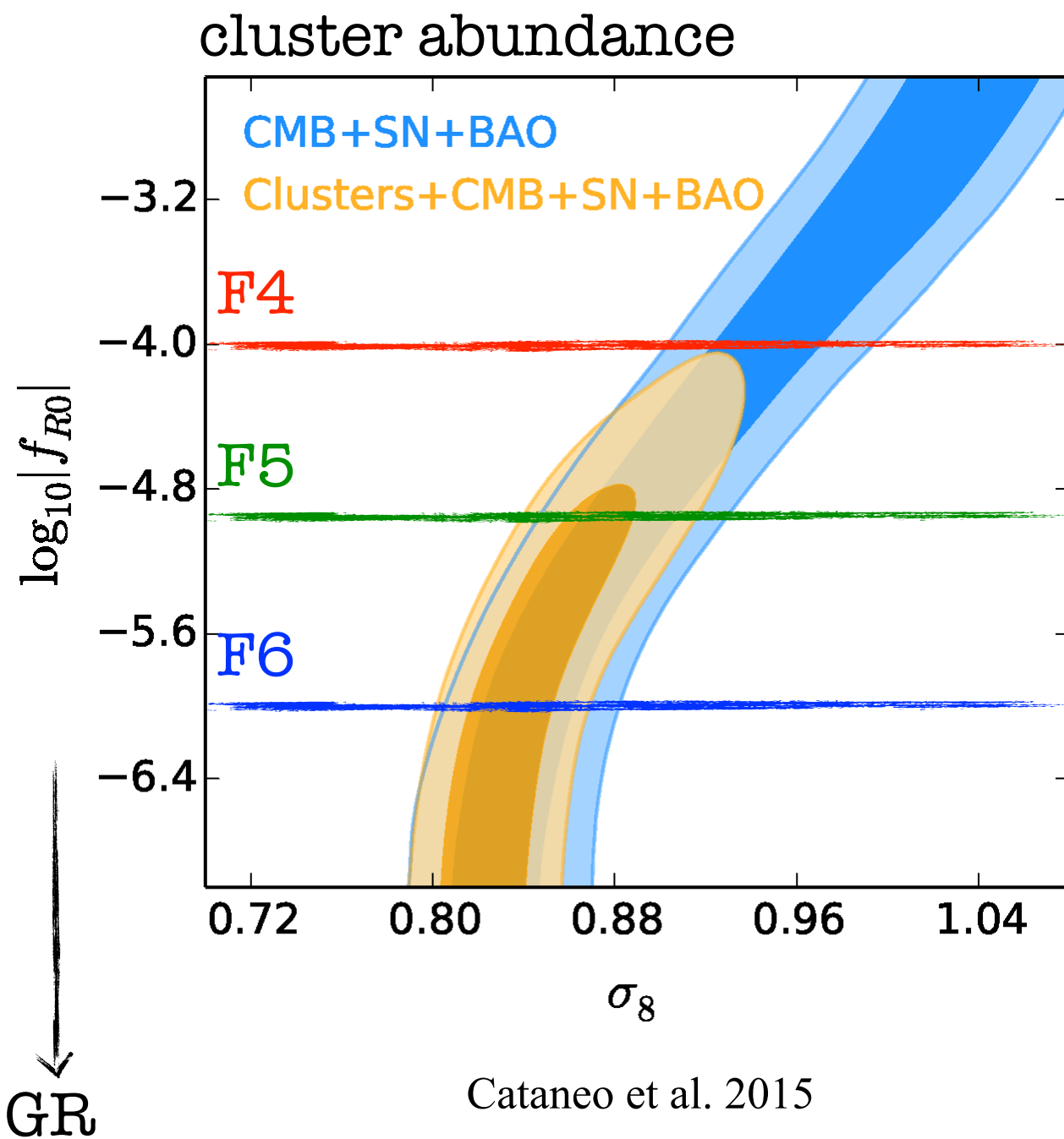
simulations give accurate predictions, but not realistic to search the model parameter space continuously. Can use fitting formulae (Lecture 3)



Testing Models using Cluster Abundance



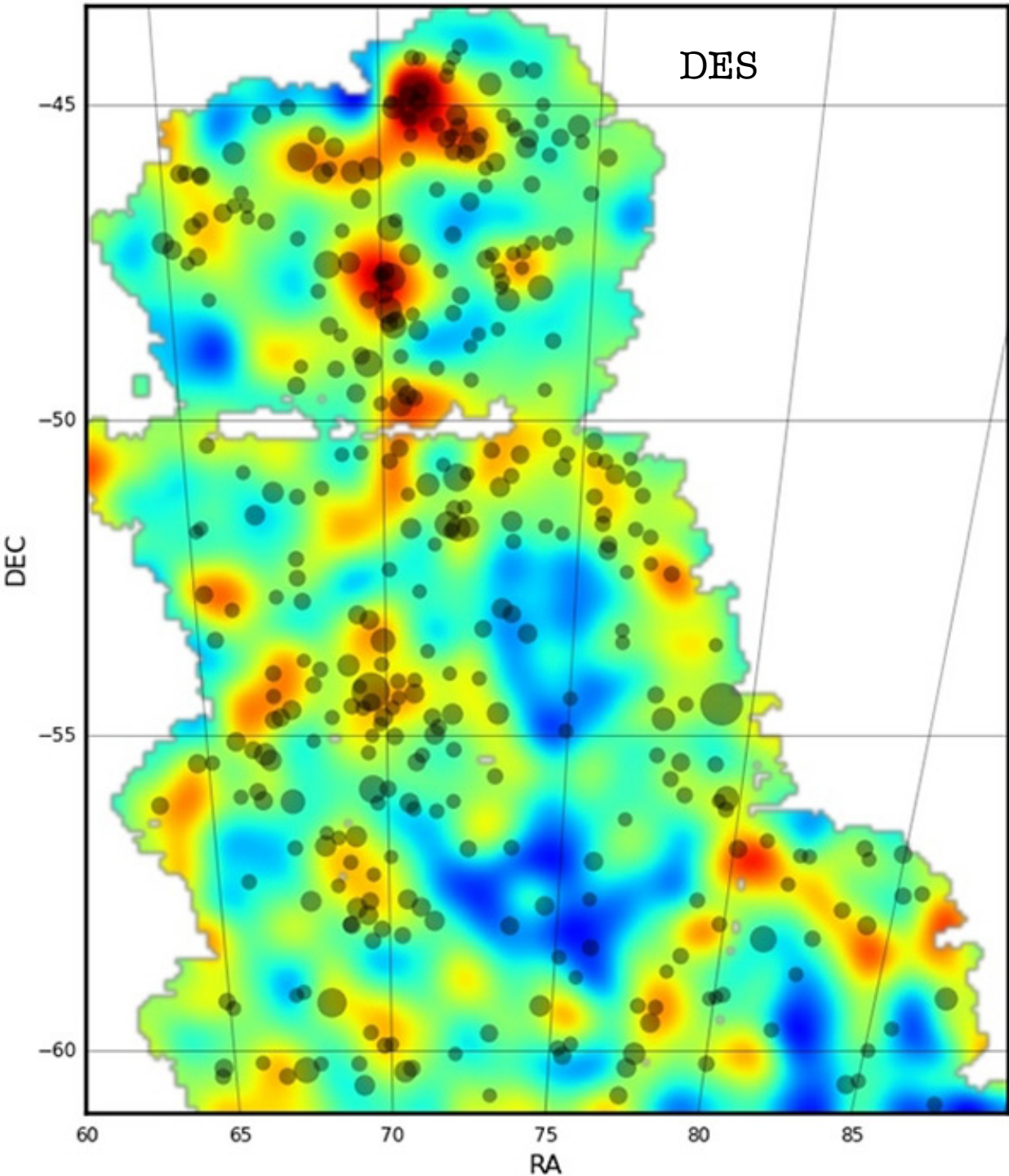
Case I Example



Even without exact prior knowledge of the parameters in the O-M relation, one can regard these parameters as part of ‘the model’, and use MCMC to search the combined parameter space consisting of theory (e.g., modified gravity) parameters plus these parameters.

Cataneo et al. 2015 used this method to place strong constraint on $f(R)$ gravity [left]

Case 2 Example

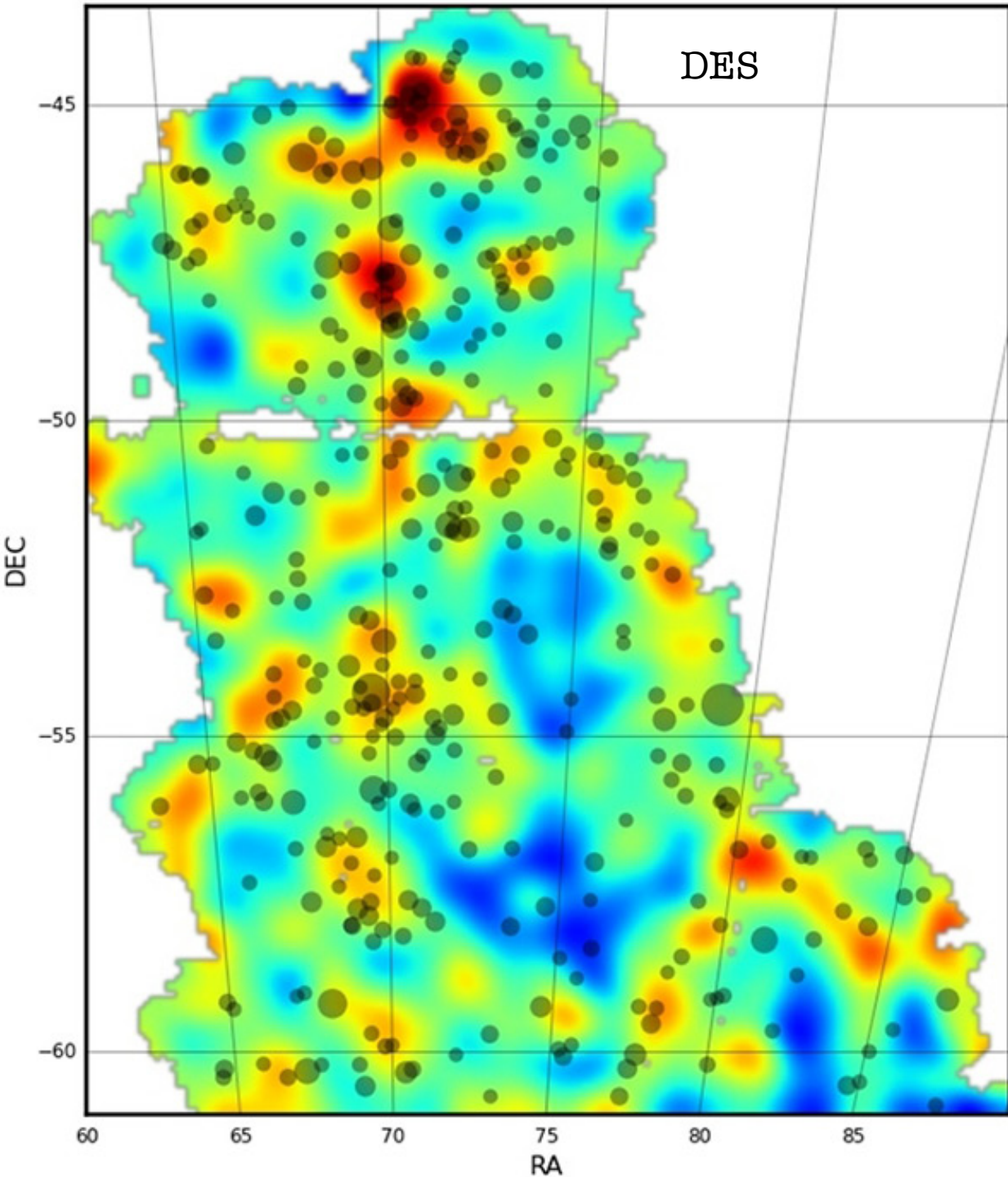


In some cases, we may have a good model for the relation between cluster observable and cluster mass.

One such example of cluster observable is the weak lensing peak counts.

WL peaks are regions in the lensing map where lensing effect is strong, and they generally correspond to large clusters.

Case 2 Example

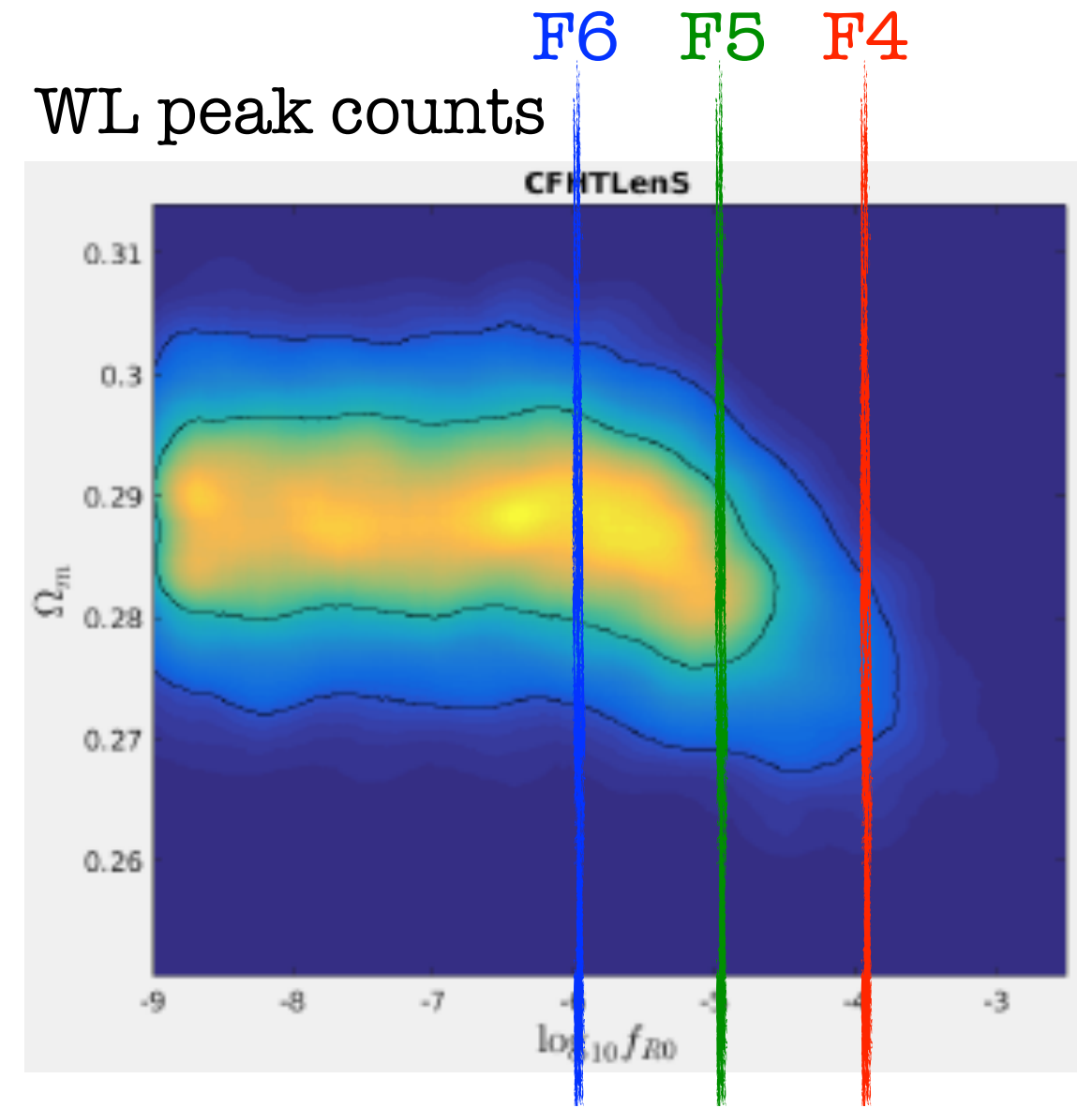
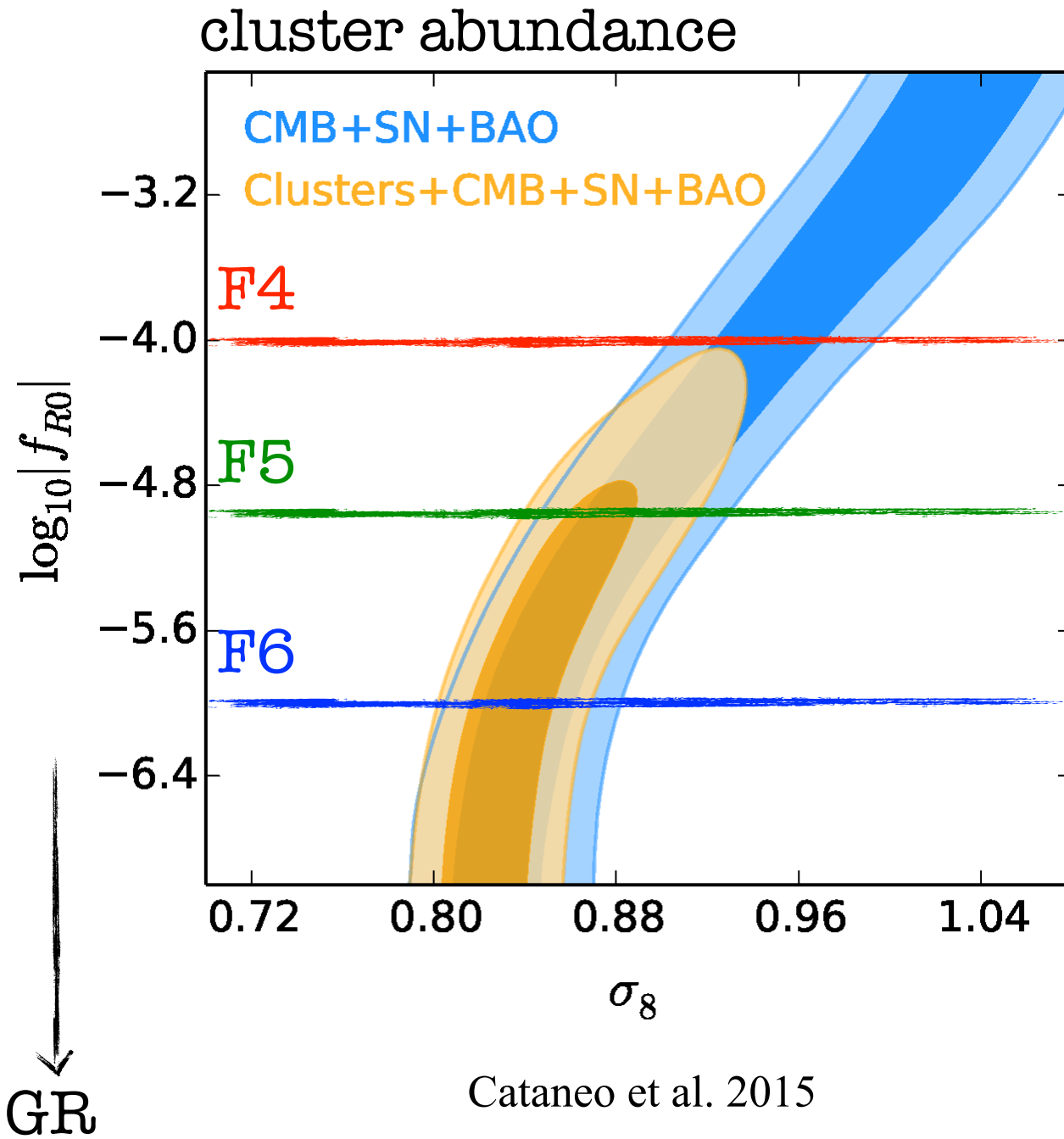


There are models which can connect the abundance of such peaks to halo abundance (verified by mock data).

In the case of $f(R)$ gravity, modified gravity does not affect the trajectories of photons, and so the model is expected to work as well (verified by mock data).

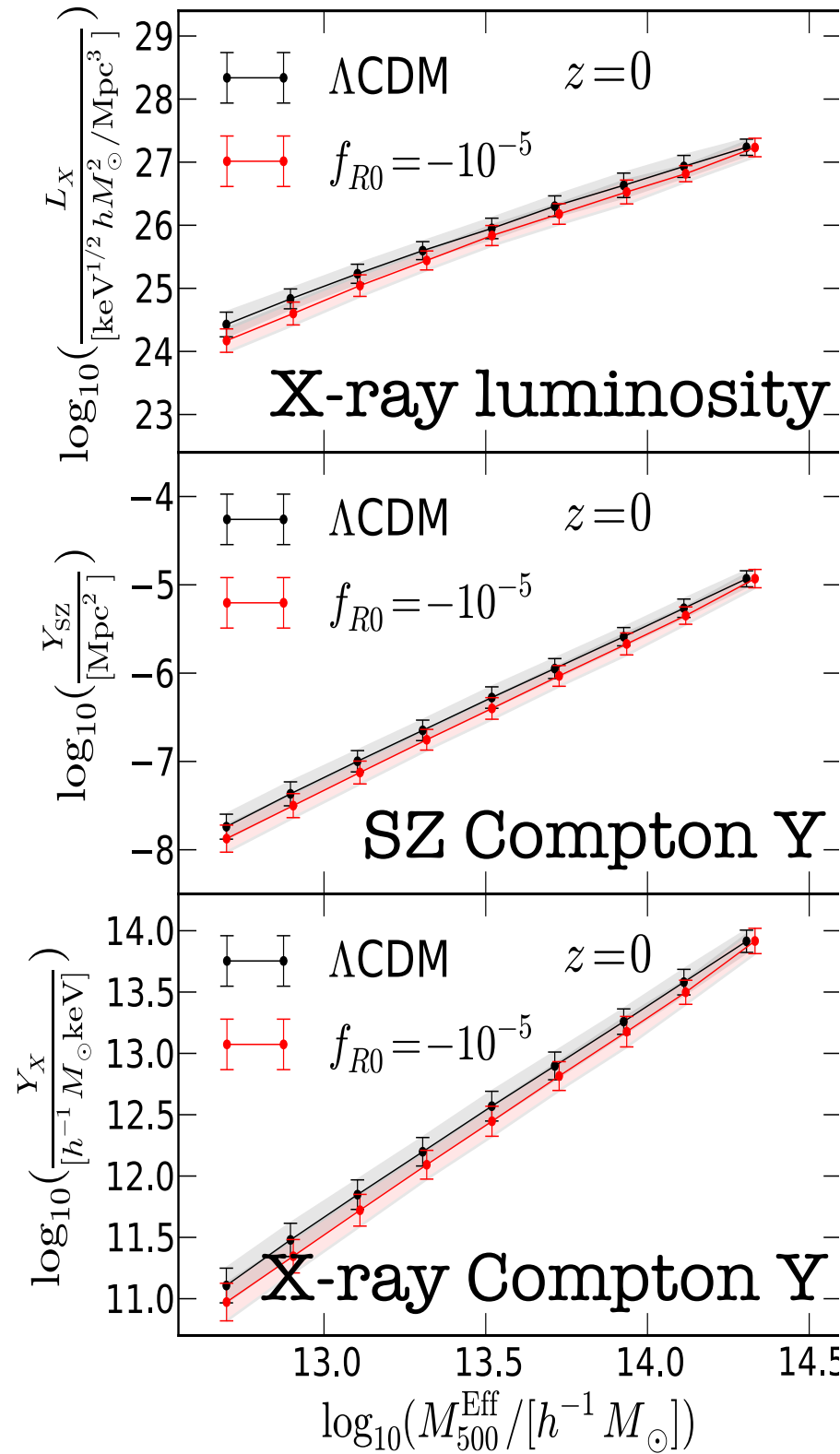
This method has the advantage that lensing is overall effect, and less affected by baryon physics

Case 2 Example



This method gives very strong constraints on the $f(R)$ model.

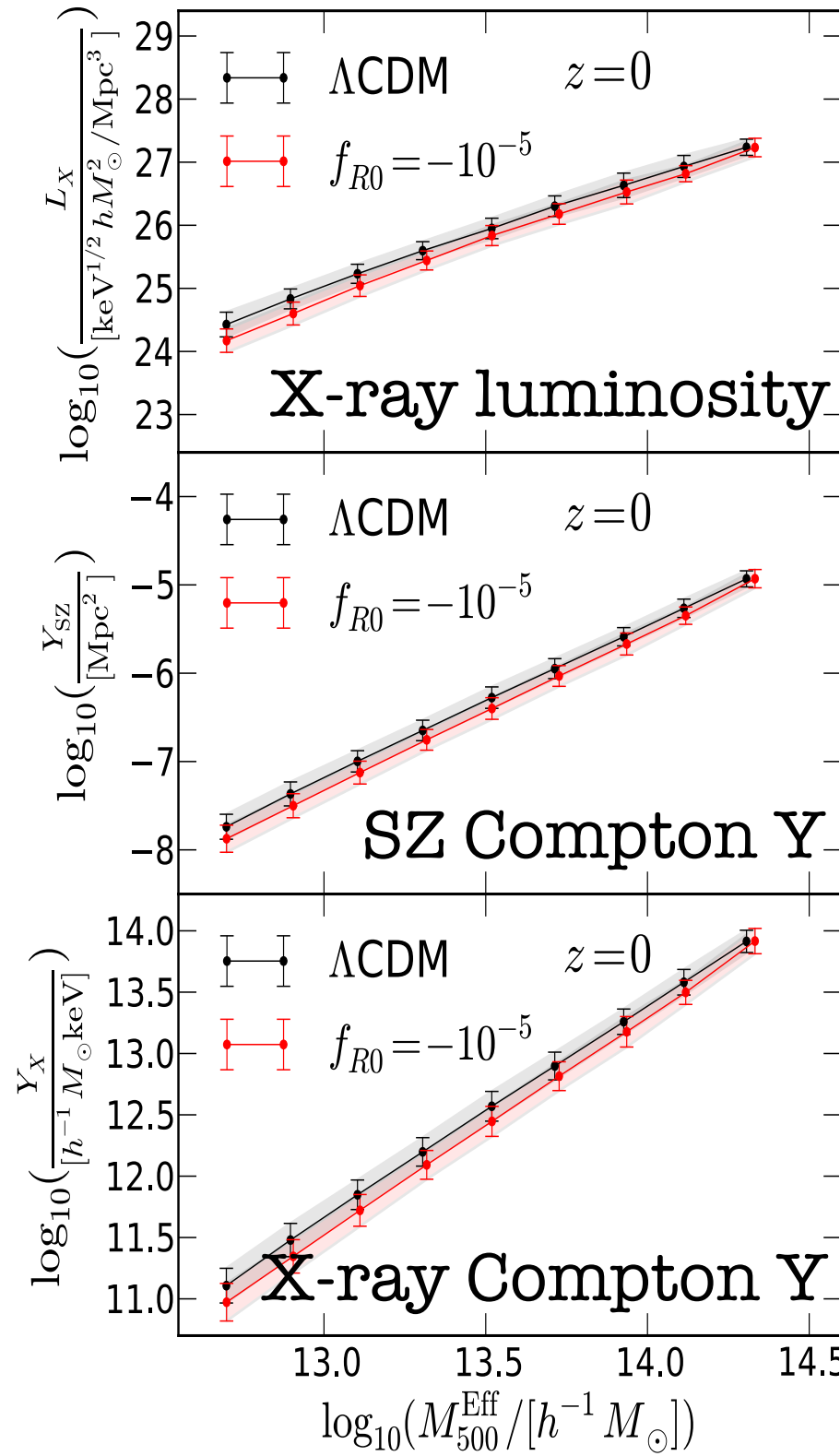
Case 3 Example



In many other cases, we may have a good knowledge of the relation between certain cluster observables and the cluster's mass (for example, these can be learned from hydrodynamical simulations) for the LCDM model.

However, naively, such relations are not work for nonstandard models.

Case 3 Example

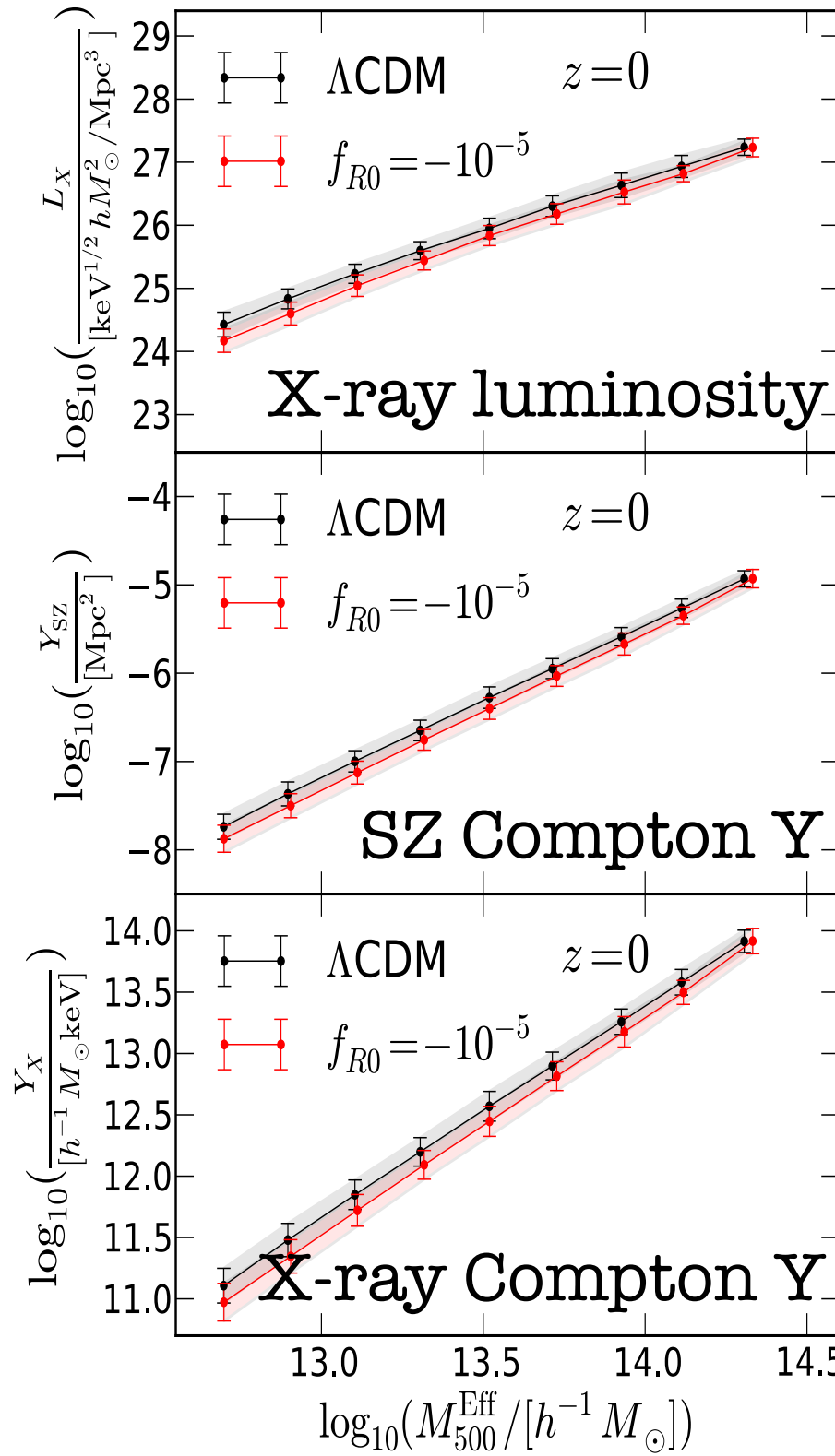


$$L_X(< r) = \int_0^r dr 4\pi r^2 \rho_{\text{gas}}^2 T_{\text{gas}}^{1/2}$$

$$Y_{\text{SZ}}(< r) = \frac{\sigma_T}{m_e c^2} \int_0^r dr 4\pi r^2 P_e$$

$$Y_X(< r) = \bar{T}_{\text{gas}} \int_0^r dr 4\pi r^2 \rho_{\text{gas}}$$

Case 3 Example



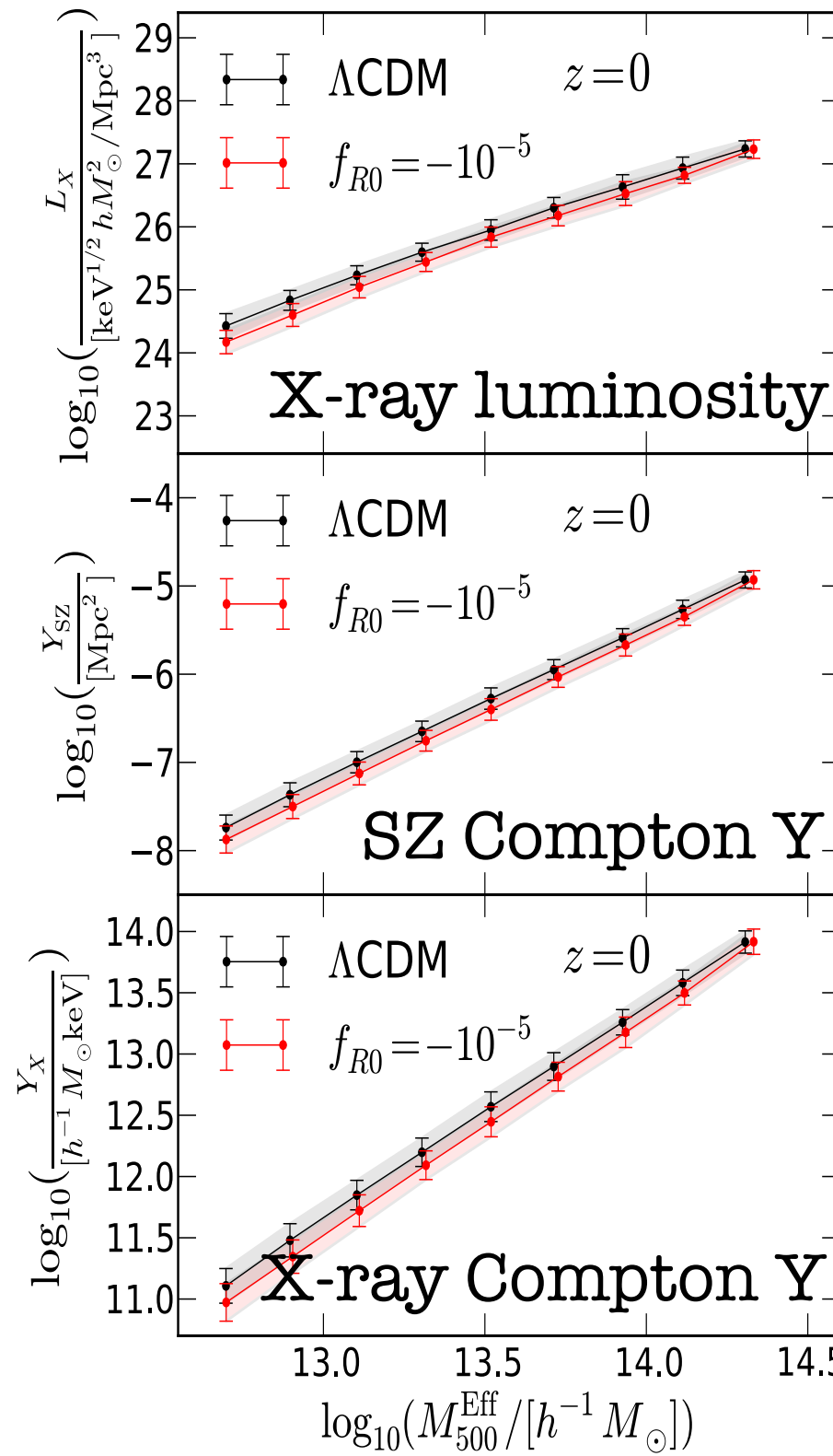
$$\begin{aligned}\nabla^2 \Phi &= 4\pi G \delta \rho_m + \beta(\varphi) \nabla^2 \varphi \\ &\equiv 4\pi G \delta \rho_{m,eff}\end{aligned}$$

gravity

baryons

$$Y_X(< r) = \bar{T}_{\text{gas}} \int_0^r dr 4\pi r^2 \rho_{\text{gas}}$$

Case 3 Example



treat the haloes in modified gravity
as Λ CDM haloes of rescaled baryon
fraction (by $M_{\text{true}}/M_{\text{eff}}$)

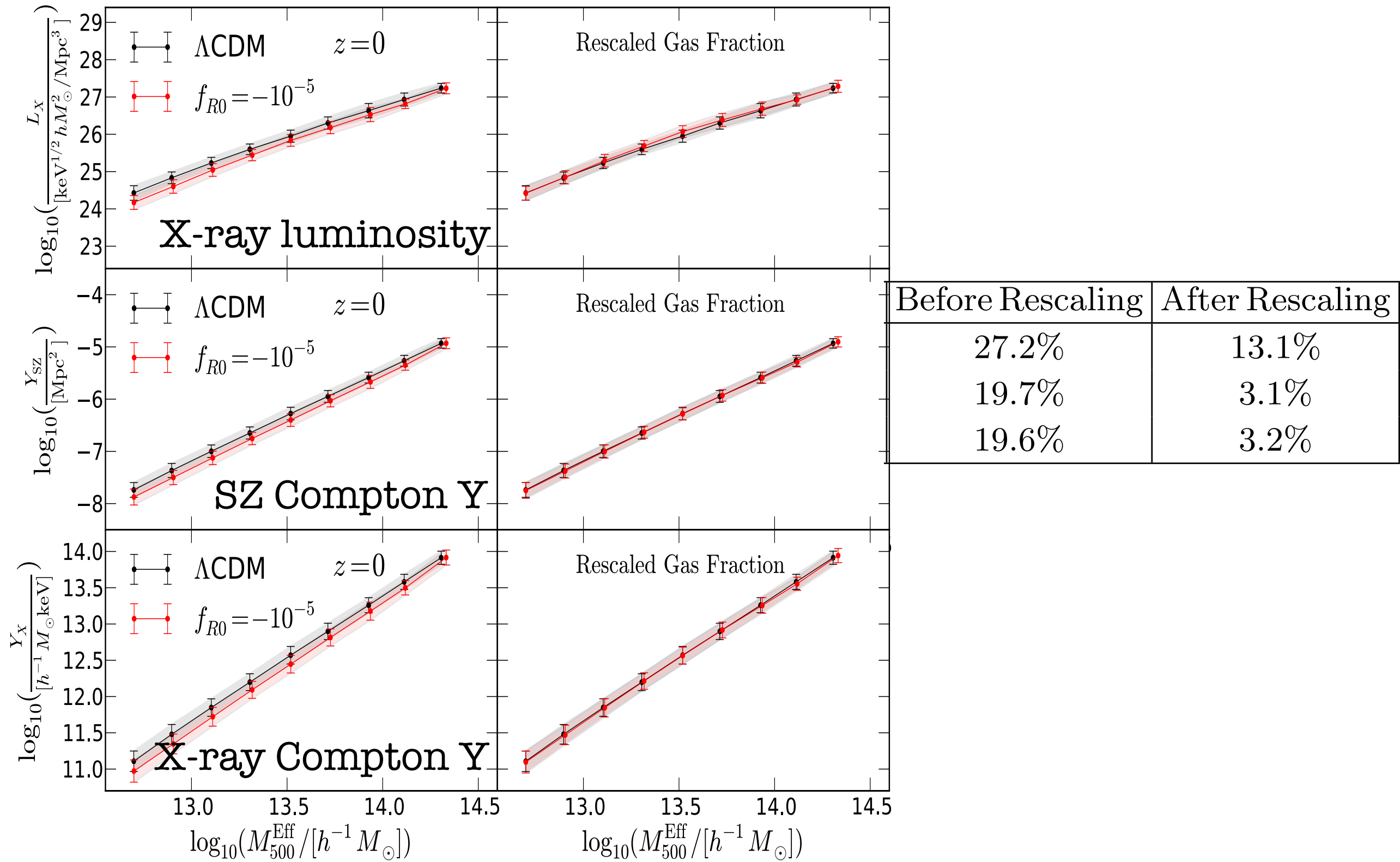
$$\begin{aligned}\nabla^2 \Phi &= 4\pi G \delta \rho_m + \beta(\varphi) \nabla^2 \varphi \\ &\equiv 4\pi G \delta \rho_{m,\text{eff}}\end{aligned}$$

gravity

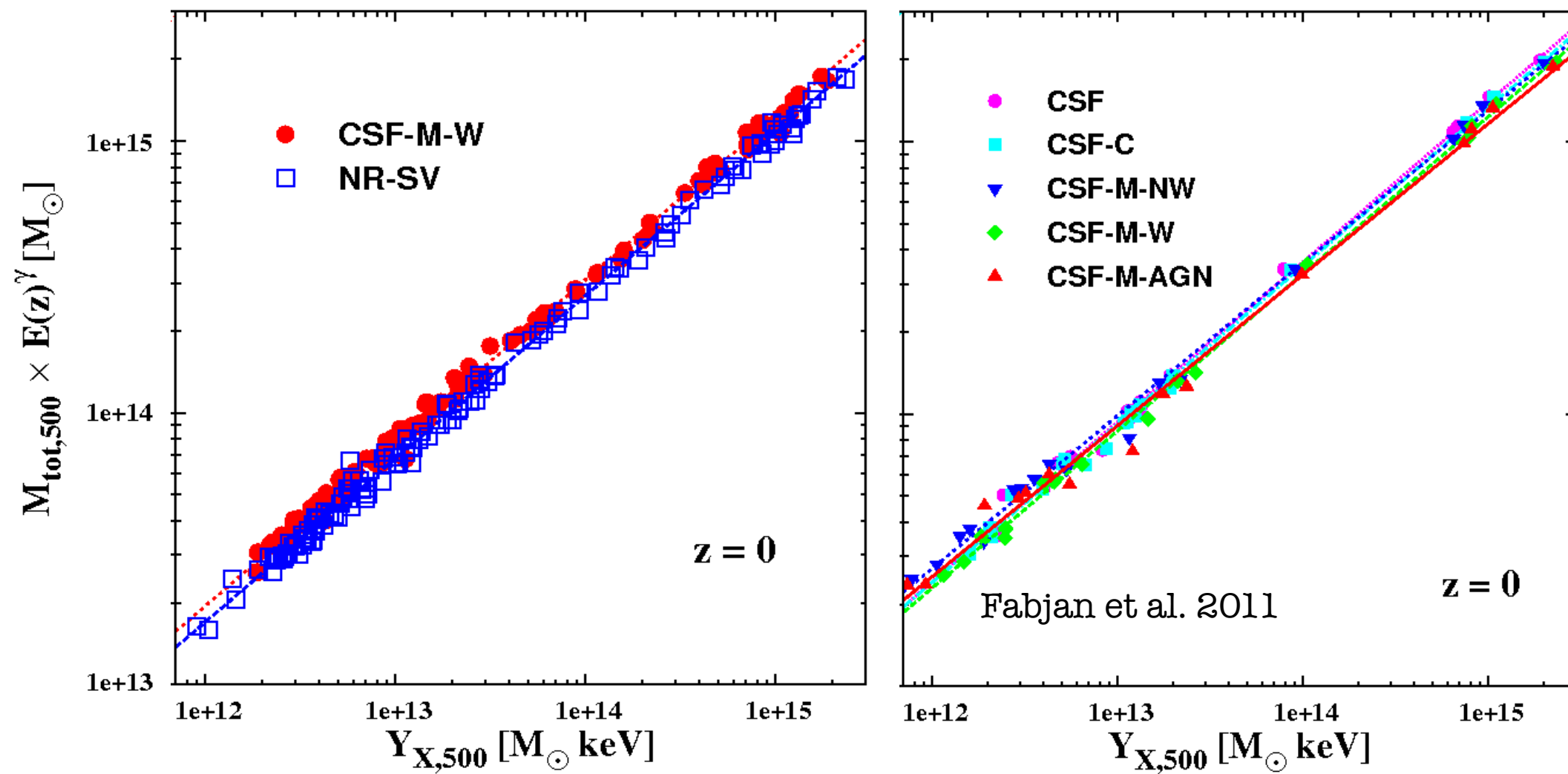
baryons

$$Y_X(< r) = \bar{T}_{\text{gas}} \int_0^r dr 4\pi r^2 \rho_{\text{gas}}$$

Case 3 Example

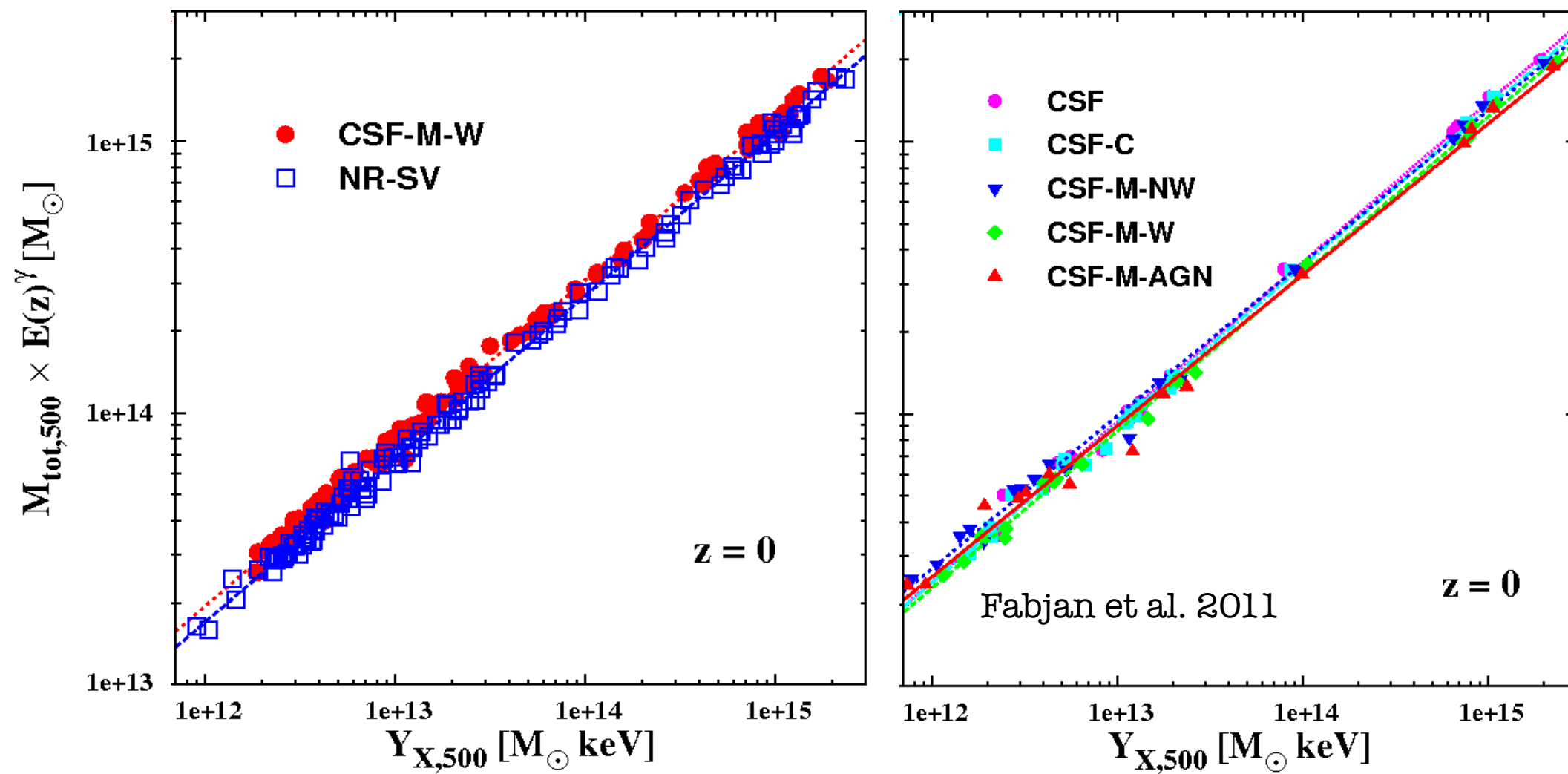


Case 3 Example



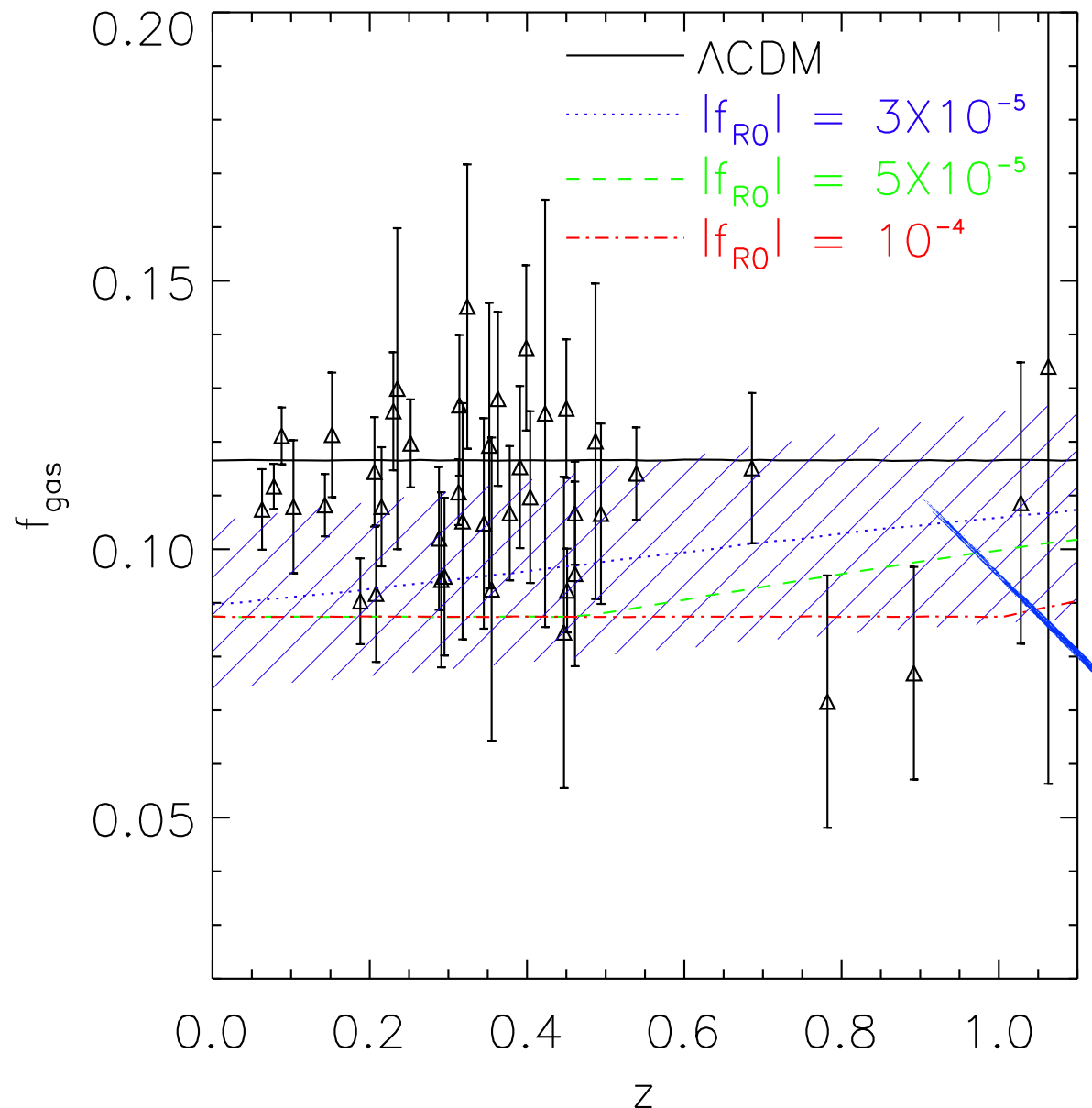
Uncertainty in galaxy formation affects scaling relations to the level of $\sim 15\%$, much larger than the 3% error in the above method

Case 3 Example



This can be an efficient way to find O-M relations in nonstandard models using the knowledge for LCDM, without having to do very expensive hydro simulations for nonstandard models

Cluster Gas Fraction as a Cosmological Test



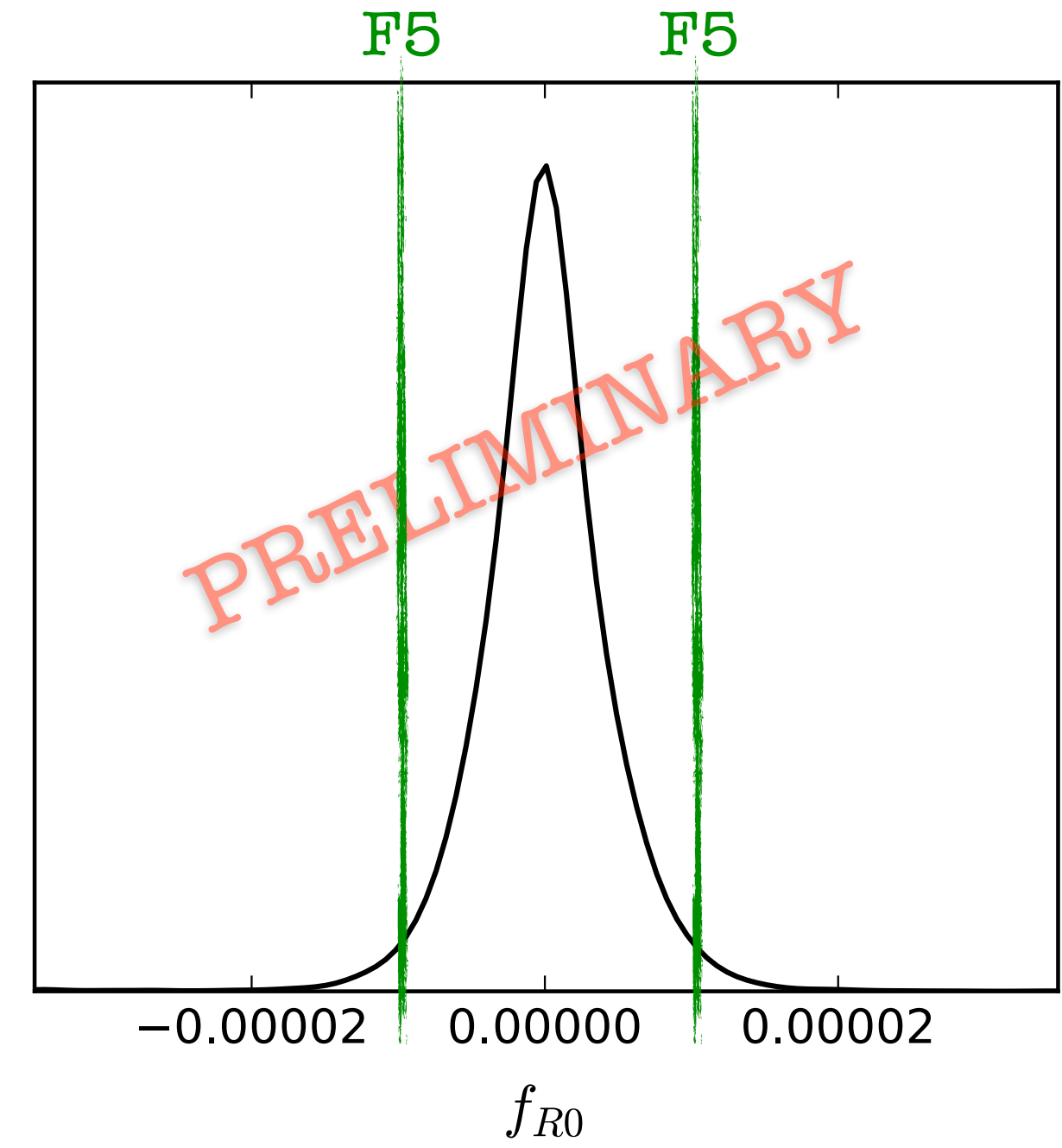
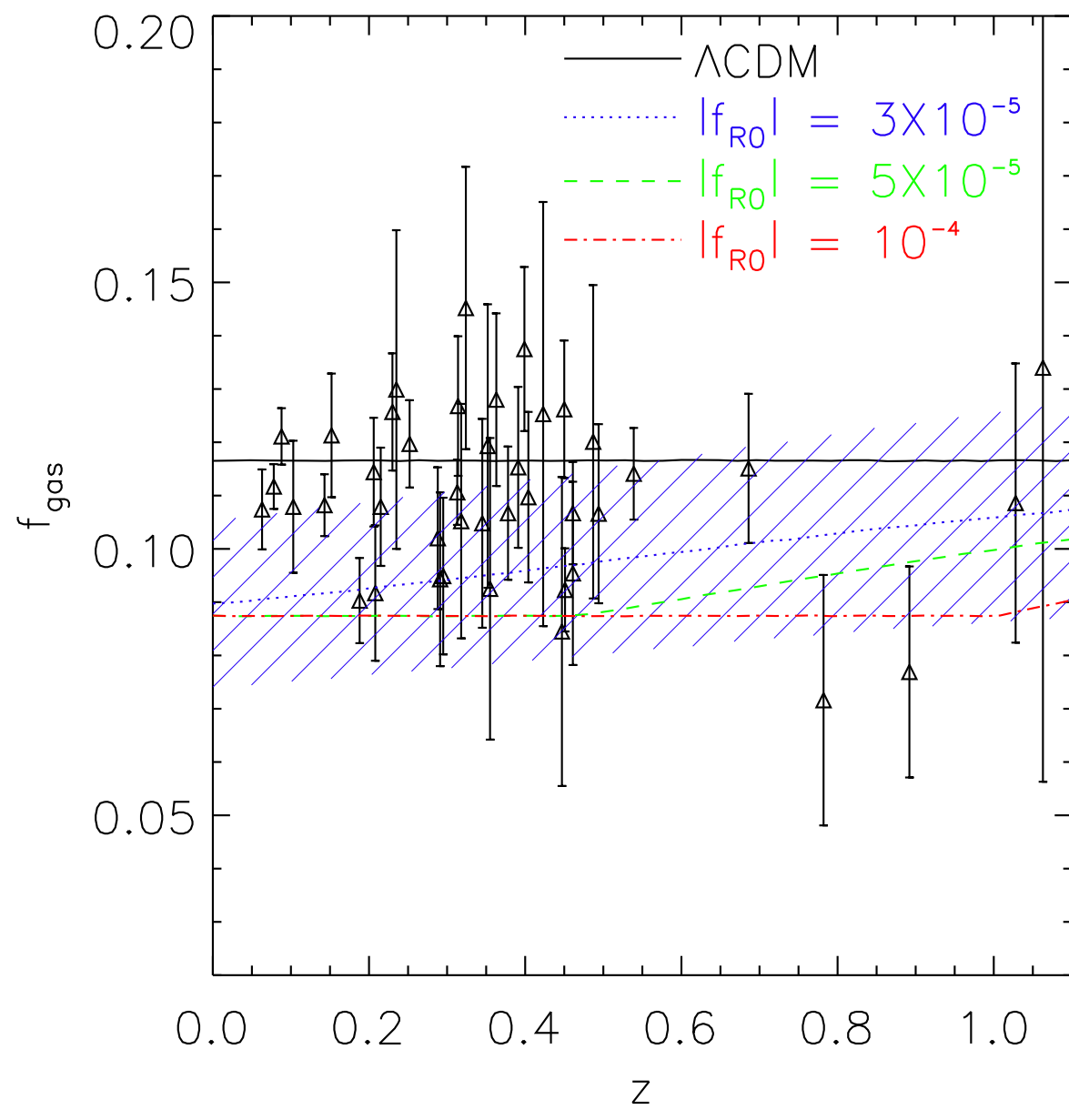
symbols: data for 42 clusters
from Allen et al. 2008

black line: LCDM

coloured lines: $f(R)$ gravity

systematics due to depletion,
non-thermal pressure, stars...

Cluster Gas Fraction as a Cosmological Test



Summary

- Nonstandard models exist to explain the cosmic acceleration, as the standard model has no solid theoretical foundation.
- Parameterisations can be used to enable more efficient studies of the nonstandard models.
- Simulations are a useful and accurate tool to make theoretical predictions.
- Connections to observations can be made to allow model constraints. Promising results already exist.
- Future observations will further improve this situation. But more needs to be done.